

Overview of LNT Modeling Approaches



Miloš Marek, Petr Kočí

<http://www.vscht.cz/monolith>

CLEERS Workshop 2012-05-02

Contents

- NO_x storage and reduction principles
- Monolith channel model
- Transport effects in coated catalytic layer
- Global kinetics, microkinetics
- Reaction mechanisms – NO_x storage
- Reaction mechanisms – reduction of the stored NO_x
- Selectivity issues – NH_3 and N_2O
- Conclusions

NSRC – NO_x storage and reduction catalyst = LNT – Lean NO_x trap

Three way catalyst + NO_x adsorbing components

Toyota JSAE 946 (1994) 41-44. - the first publication
SAE 950809, 1995
Catalysis Today **27**, 63 (1996)
Daimler Appl. Catal. B. Env. **7**, 153 (1995)

NM / EA / OS / γ – Al₂O₃

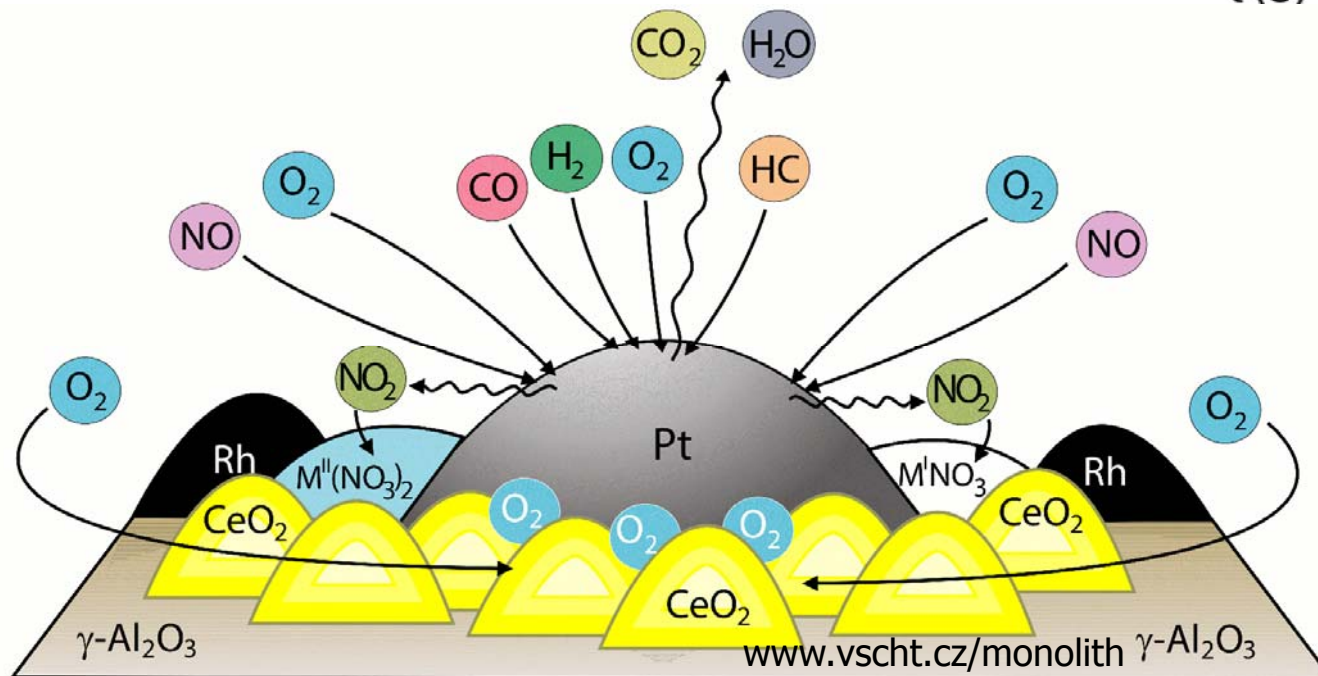
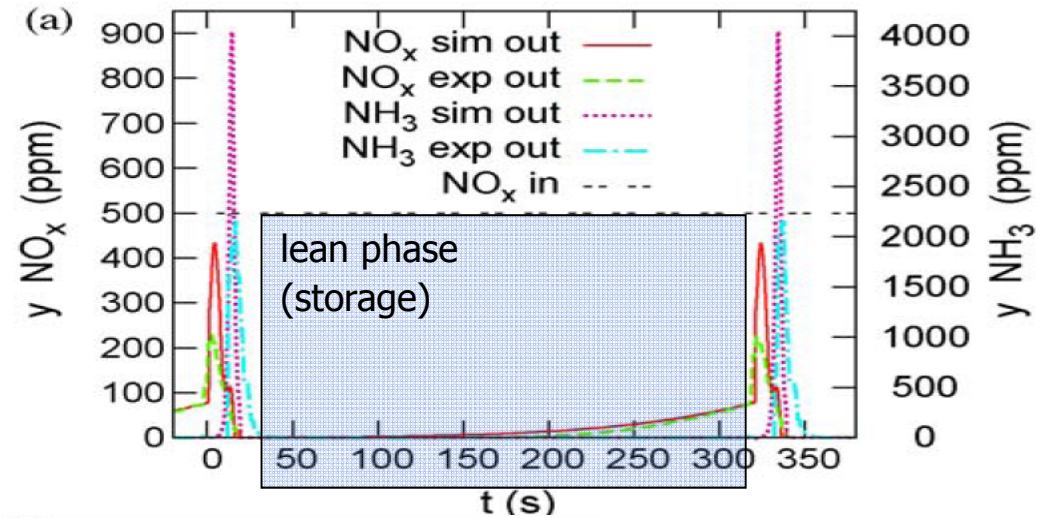
NM noble metals: Pt, Rh, Pd – redox sites

EA earth alkaline and/or alkali metals: Ba, K... – NO_x storage sites

OS oxygen storage components: Ce, Zr

NO_x storage catalyst – lean fuel mixture, oxidising conditions

CO & HC oxidation
 NO oxidation to NO₂
 NO_x storage
 Oxygen storage

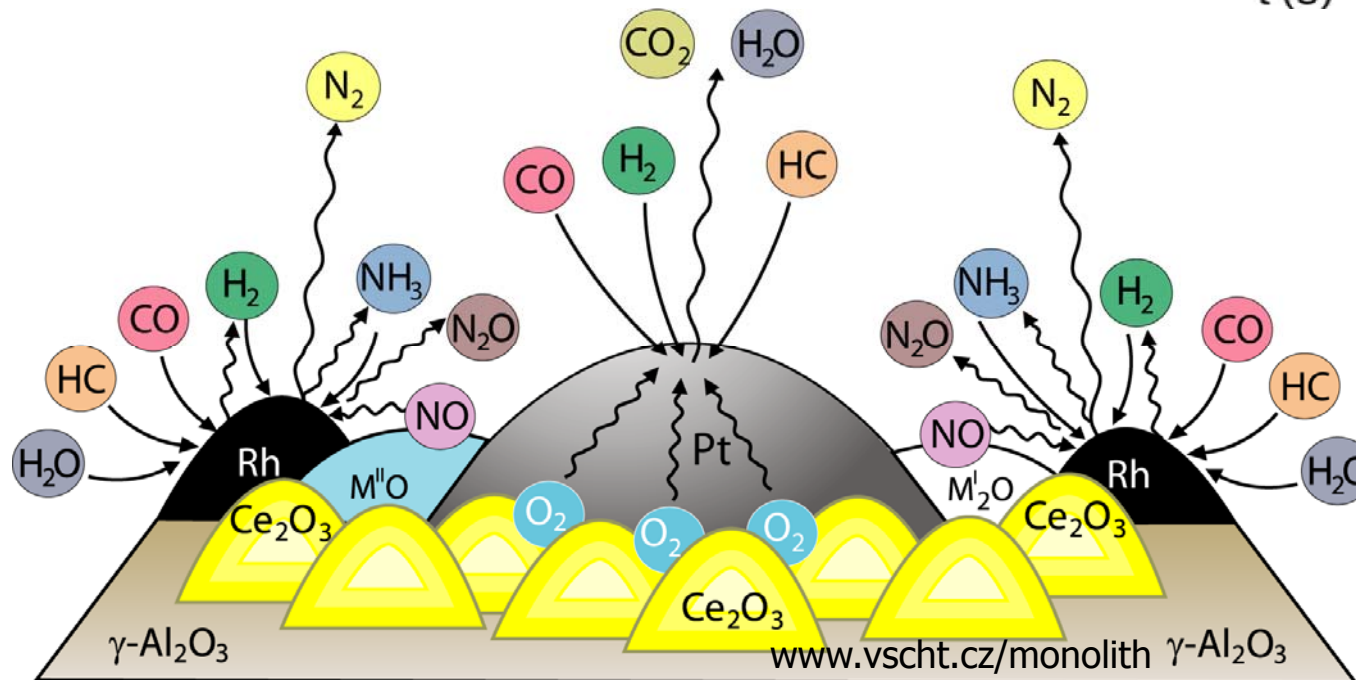
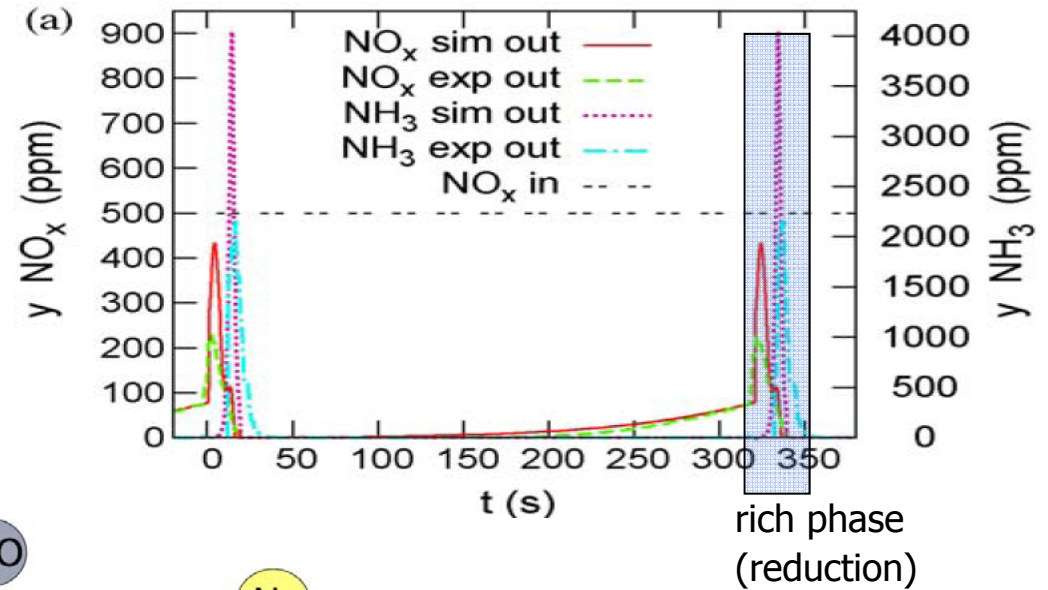


NO_x storage catalyst – rich fuel mixture, reducing conditions

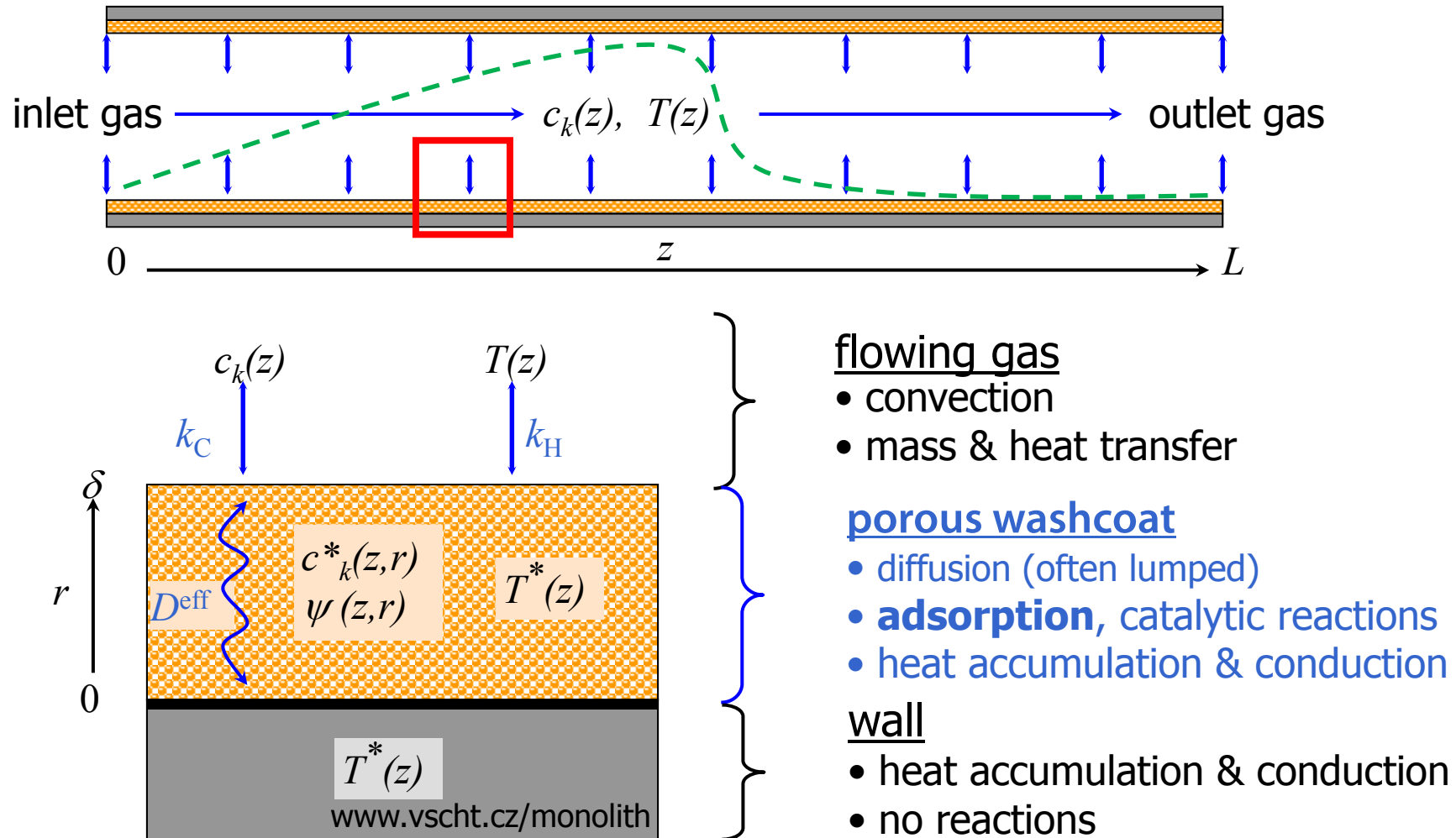
- NO_x desorption
- NO_x reduction
- Water gas shift & steam reforming
- NH₃ formation
- NH₃ oxidation
- Oxygen release

Range of NO_x reduction products:

N₂, NH₃, N₂O + desorbed NO_x



Coupling of reaction and transport – monolith channel model



⇒ Standard 1D, or 1D+1D dynamic models commonly used

⇒ **Transient solution of key adsorbed species necessary** (no steady state)

Mathematical model of monolith channel - 1D+1D washcoat

flowing gas
mass balance

$$\frac{\partial c_k(z,t)}{\partial t} = -\frac{\partial(uc_k)}{\partial z} - k_C(z)\frac{a}{\varepsilon}(c_k - c_k^*|_\delta)$$

washcoat pores
mass balance

$$\varepsilon^* \frac{\partial c_k^*(z,r,t)}{\partial t} = D^{\text{eff}} \frac{\partial^2 c_k^*}{\partial r^2} + \sum_{j=1}^J v_{k,j} R_j$$

catalytic surface
mass balance

$$\frac{\partial \psi_m(z,r,t)}{\partial t} = \frac{1}{\Psi_{\text{cap},m}} \sum_{j=1}^J v_{m,j} R_j$$

flowing gas
enthalpy balance

$$\rho c_p \frac{\partial T(z,t)}{\partial t} = -u\rho c_p \frac{\partial T}{\partial z} - k_H(z)\frac{a}{\varepsilon}(T - T^*)$$

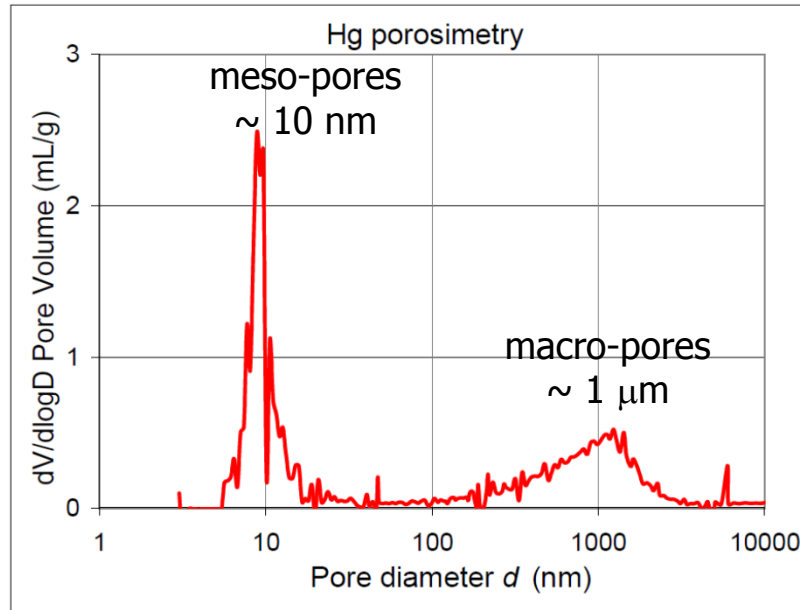
solid phase
enthalpy balance

$$\rho^* c_p^* \frac{\partial T^*(z,t)}{\partial t} = \lambda_z^* \frac{\partial^2 T^*}{\partial z^2} - a \sum_{j=1}^J \Delta H_{R,j} \int_{r=0}^{\delta} R_j dr + k_H(z,t)\frac{a}{1-\varepsilon}(T - T^*)$$

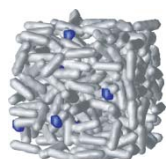
+ respective **boundary & initial conditions**

Effective diffusivity in coated catalyst layer

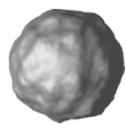
Bimodal pore-size distribution



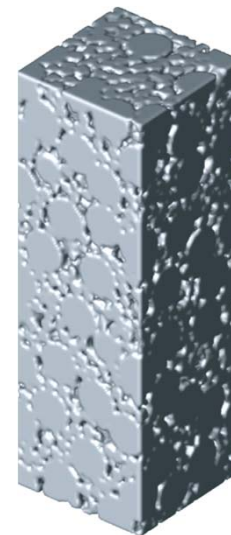
Macropores enable relatively fast transport through the layer (volume diffusion), in contrast to small mesopores (Knudsen diffusion). Neglect of macropores contribution leads to severe overestimation of diffusion limitations.



Pt/γ-Al₂O₃
nano-scale, pores ~10 nm



Pt/γ-Al₂O₃
micro-particle



coated Pt/γ-Al₂O₃
pores ~ 1 μm

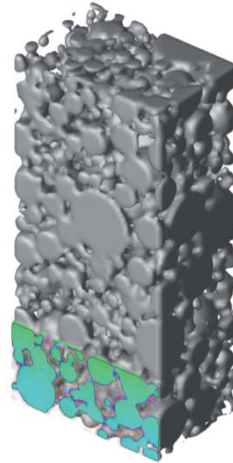
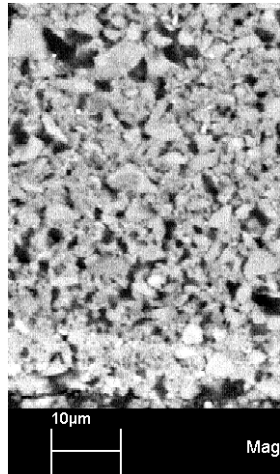
3D digital reconstruction techniques and multi-scale modeling can be used for precise evaluation of diffusion in porous catalytic coating.

Novák et al., Multi-scale modelling and measurements of diffusion through porous catalytic coatings: An application to exhaust gas oxidation, Catalysis Today (2012), in press.

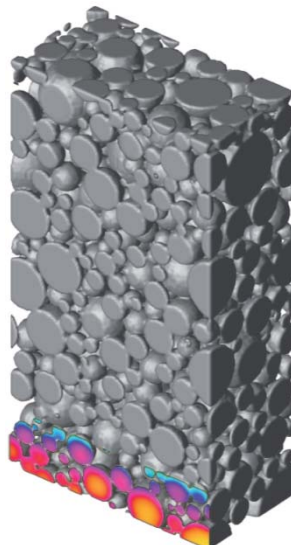
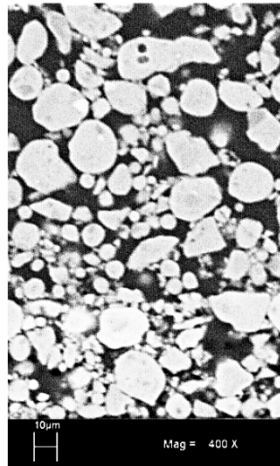
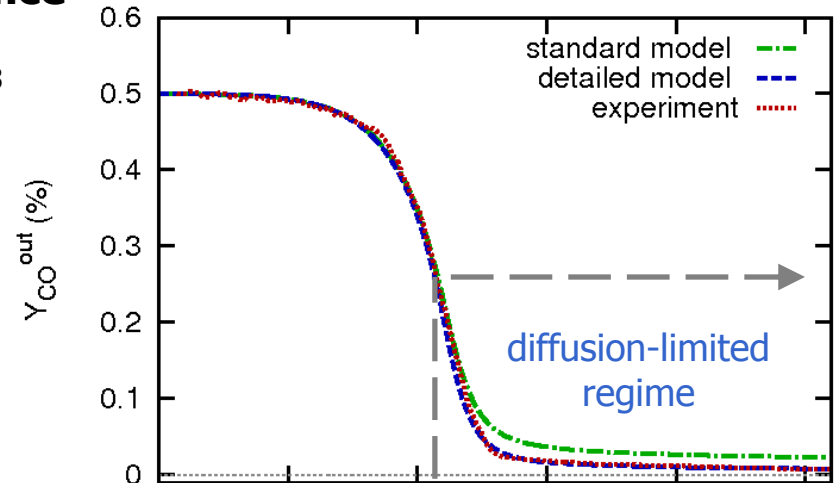
+ **CLEERS** poster

Internal diffusion in multi-layer coatings (e.g. LNT/SCR, ASC)

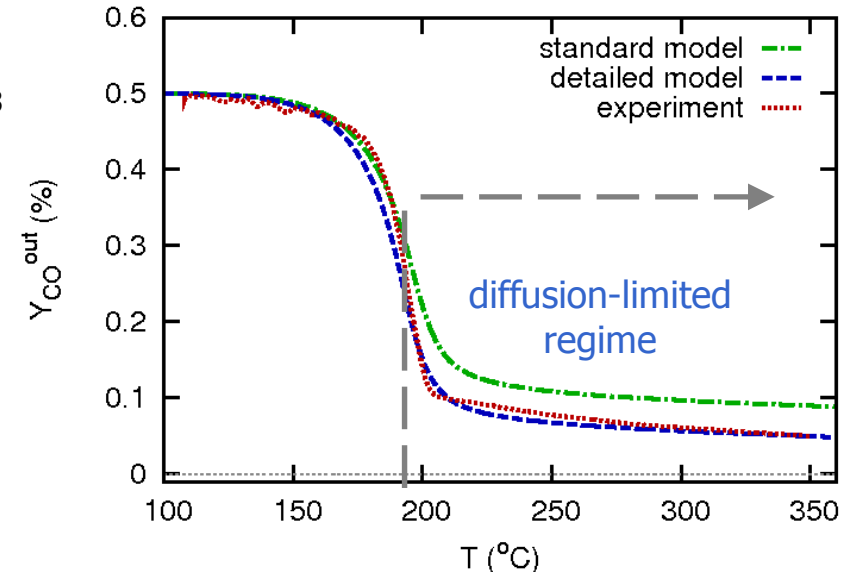
Considerable effect on catalyst performance



Coated $\gamma\text{-Al}_2\text{O}_3$
 $d_{90}=7\ \mu\text{m}$;
 top inert layer
 $50\ \mu\text{m}$;
 Bottom active
 layer $15\ \mu\text{m}$;
 $\varepsilon^M=26\ \%$



Coated $\gamma\text{-Al}_2\text{O}_3$
 $d_{90}=22\ \mu\text{m}$;
 top inert layer
 $240\ \mu\text{m}$;
 Bottom active
 layer $40\ \mu\text{m}$;
 $\varepsilon^M=36\ \%$



Novák et al., Multi-scale modelling and measurements of diffusion through porous catalytic coatings: An application to exhaust gas oxidation, Catalysis Today (2012), in press.

+ **CLEERS poster**

Reaction kinetics

Activity of metal nanoparticles depends on their size and shape

Recent examples

Z. Wu et al, Journal of Catalysis 285 (2012) 61

CO oxidation activity over CeO₂ nanocrystals rods > cubes > octahedra

C. Wu et al, Journal of Catalysis 286 (2012) 88

Coverage-dependence kinetic model for NO oxidation on Pt (111);

DFT based simulations

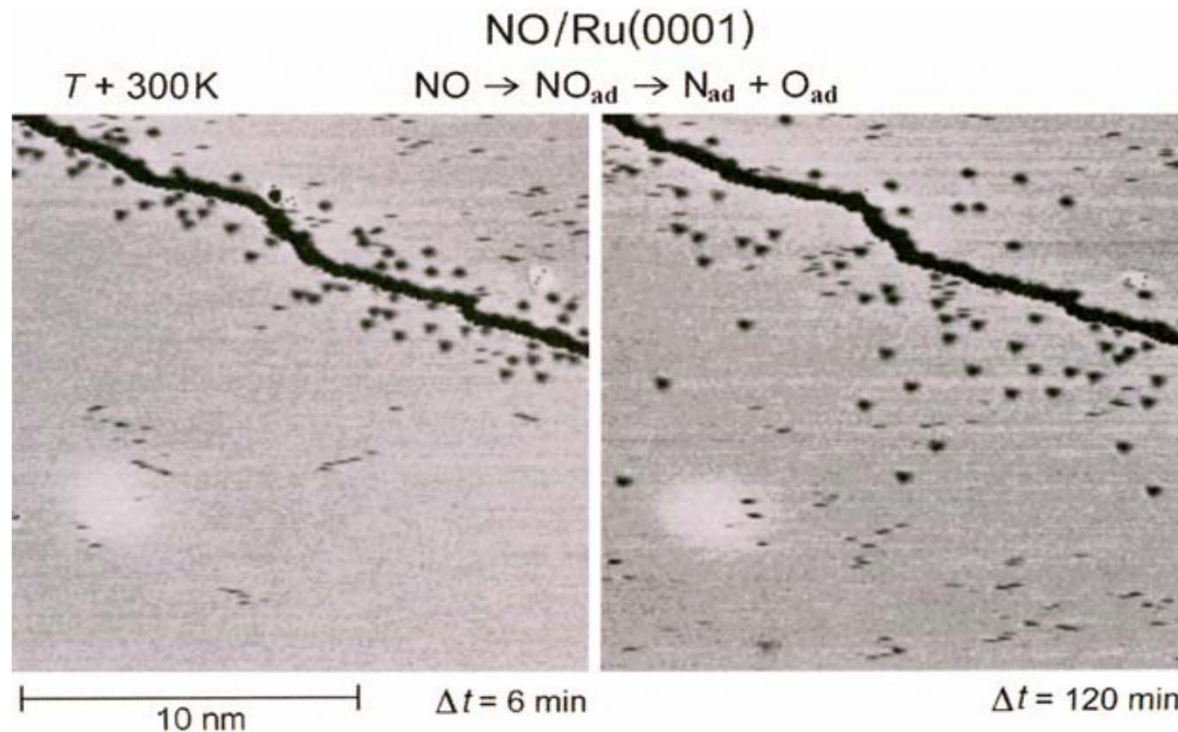
L. Lin et al Catalysis Today 175 (2011) 48

Morphology and nanosize effects of ceria on the activity for NO reduction

V. Pérez et al, Catalysis Today 180 (2012) 59

Shape-dependent catalytic activity of Pd nanoparticles

Activity of metal nanoparticles depends on their size and shape



STM images from NO interacting with a Ru(0001) surface exhibiting a monatomic step, which is, effectively, a linear array of active sites.

Zambelli, Ertl et al., Science 273 (1996), 1688.

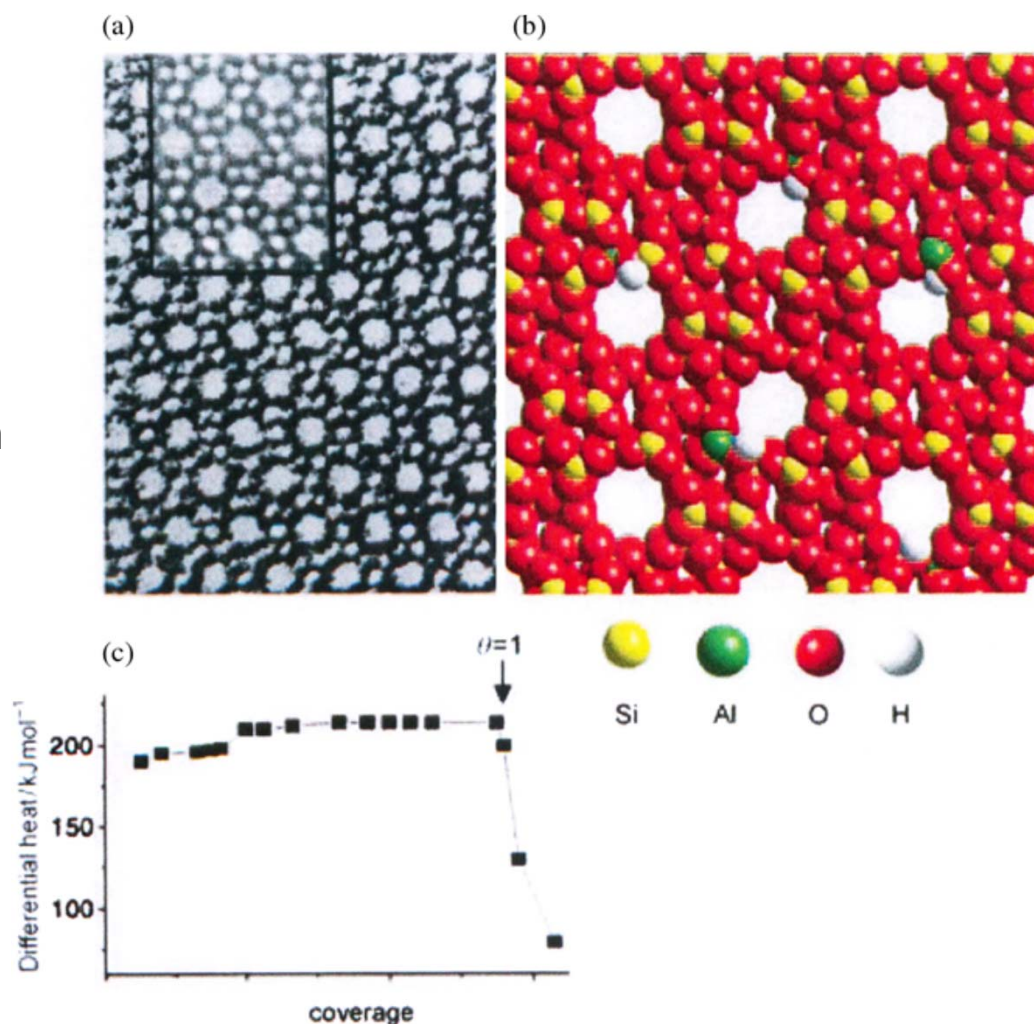
Single-site heterogeneous catalysts

Single-Site Heterogeneous Catalysts, Book by J.M. Thomas, World Scientific 2012, ISBN:978-1-84816-910-4

High-resolution electron micrograph (HREM) of H-ZSM-5 acid catalyst (Si/Al ratio *ca* 25:1). Inset shows computed image. Large white spots are pores (diameter *ca* 5.5 Å) in projection. Model of the open structure shows isolated Brønsted acid sites (loosely attached hydrogen atoms, adjacent to Al^{III} framework sites).

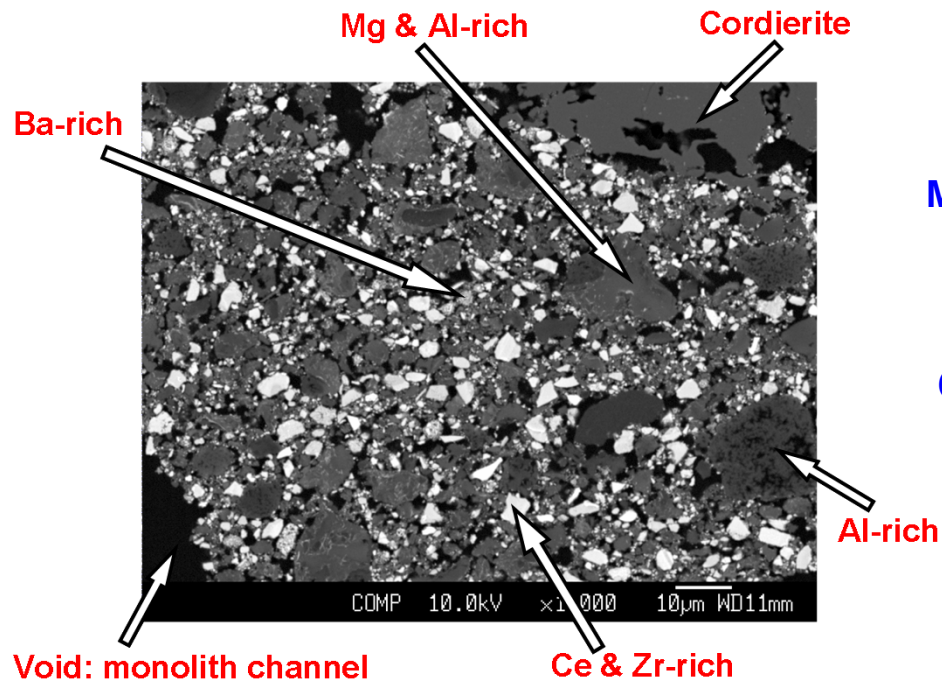
The constancy of the heat of adsorption when pyridine is titrated against the acid sites demonstrates that these sites have the same energy and same environment.

Single-site catalyst is ideal for microkinetic description.

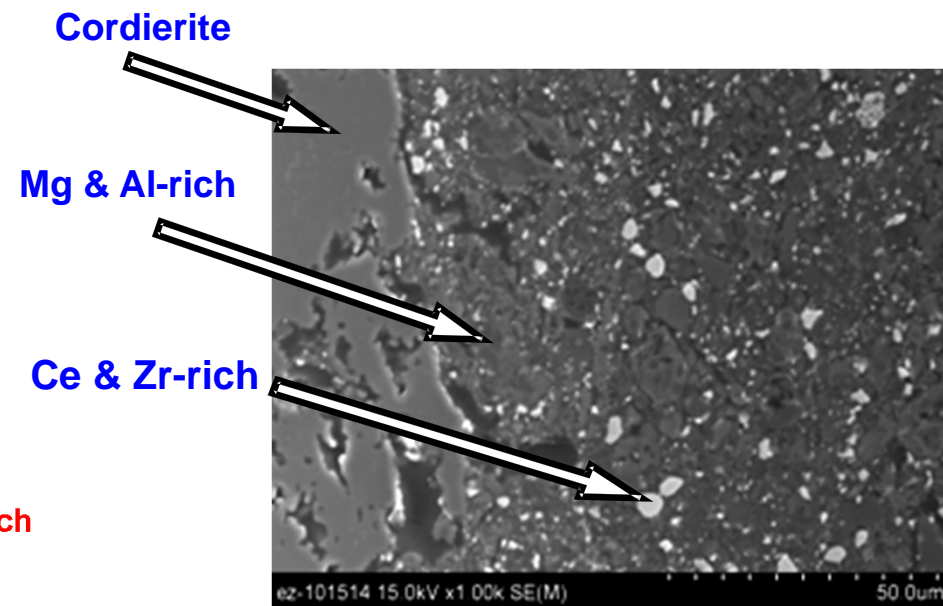


NO_x storage catalysts are not single-site catalysts (nor combination of few types of single sites)

CLEERS LNT reference 2004 (Umicore)



New CLEERS LNT 2011



Oak Ridge National Lab FEERC data

- Distribution of particle sizes of precious group metals, oxygen storage and NO_x storage material
- Mutual topology, proximity and contact between individual types of particles play important role.

Intrinsic NO_x storage mechanism

- NO₂ storage is more rapid (nitrate route, NO₂ disproportionation).
- NO can be stored as well (slower nitrite route; cf. Lietti, Nova, Forzatti et al., 2001, 2006, 2007, 2010).



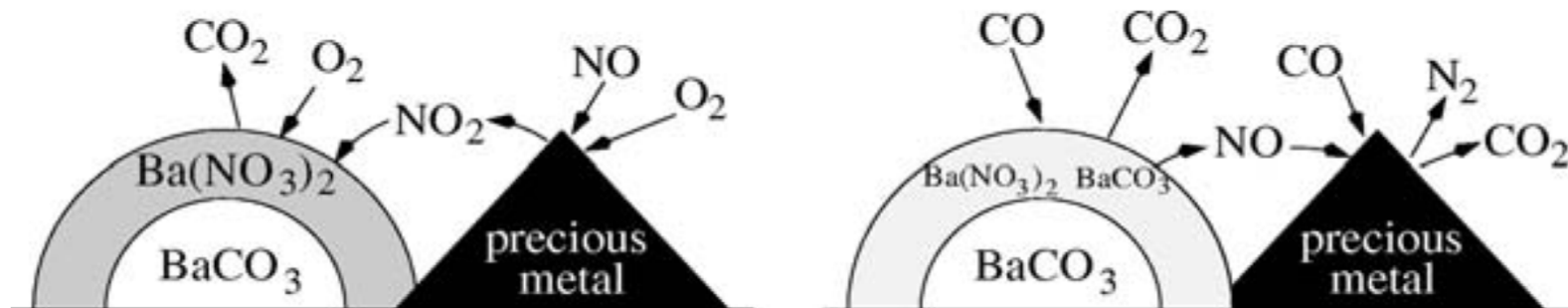
(Forzatti et al., 2010)

⇒ Gas-phase NO₂ is NOT necessary for the NO_x storage (even if it enhances the storage – NO₂ at lower T is a stronger oxidizing agent than O₂).

⇒ O₂ can oxidize nitrites to nitrates

Noble metal and NO_x storage sites topology, local transport during the storage

- a) Shrinking core model, hemispherical Ba particle, dense BaNO₃ layer on the surface blocks further transport towards the center of storage particle (e.g., Hepburn et al. 1998; Tuttlies, Schmeißer et al., 2004, 2007; Olsson et al., 2005, Scholz et al., 2007)

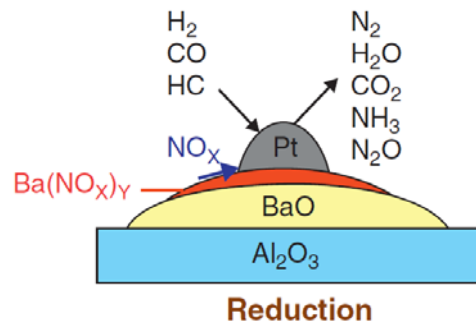
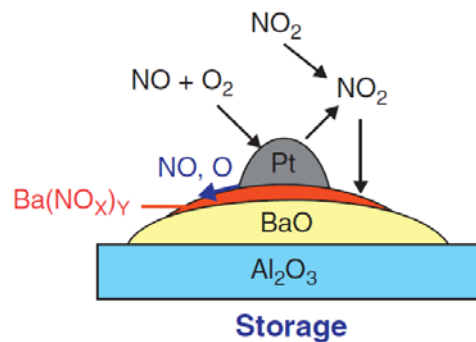


(Tuttlies et al., 2004,
Schmeißer et al., 2007)

Noble metal and NO_x storage sites topology, local transport during the storage

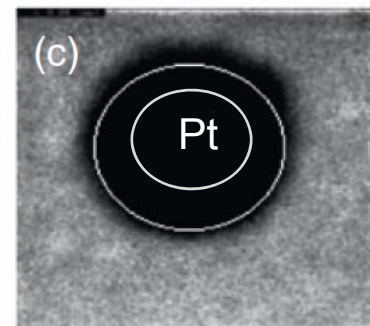
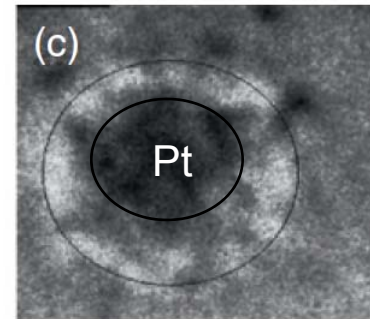
- b) Progress from easy accessible NO_x storage sites in contact with Pt sites towards more distant storage sites (e.g., Epling et al., 2007; Choi et al. 2007; Clayton, Xu, Shakya, Harold et al., 2009, 2010, 2011, 2012).

=> dispersion of Pt and contact with NO_x storage material improves the performance



(Harold et al., 2012)

SEM EPMA map of N-species

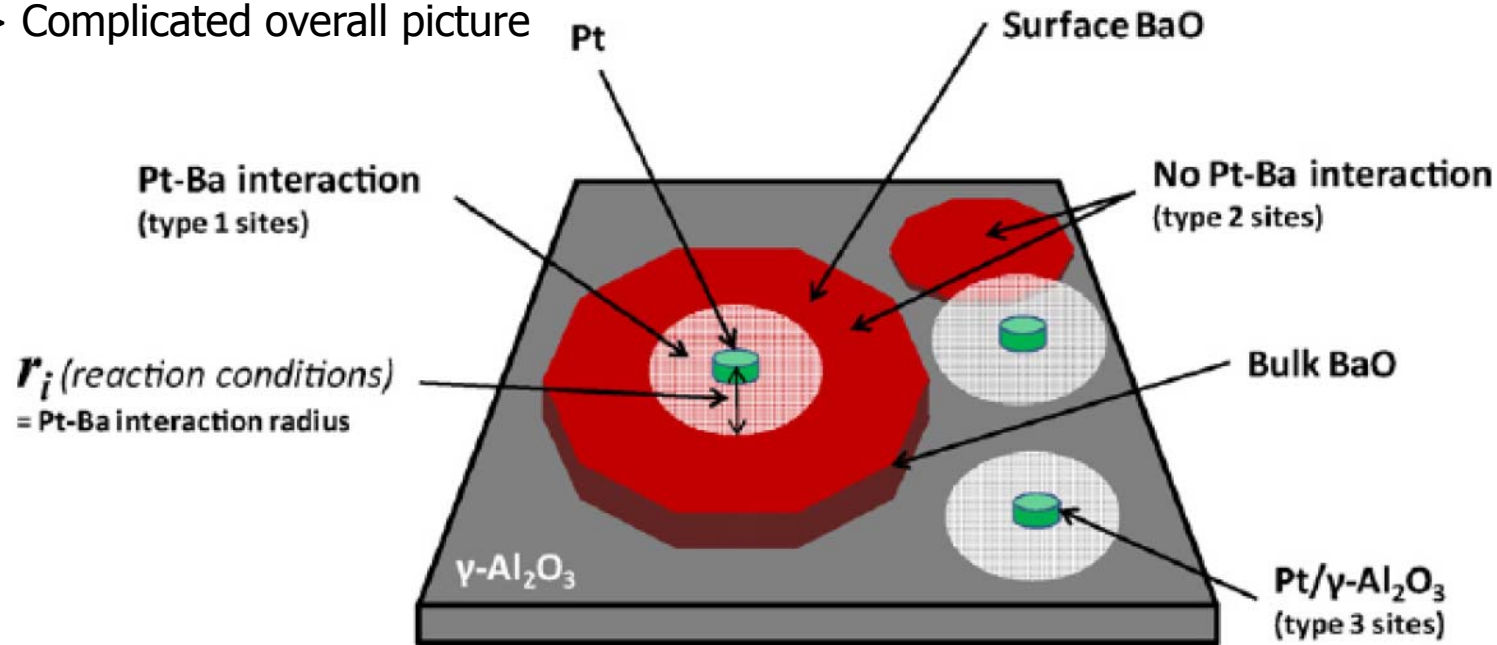


(Sakamoto et al., 2006)

Noble metal and NO_x storage sites topology, local transport during the storage

- c) NO_x can be stored also on other sites:
 - => alumina (e.g. Chaugule et al., 2010)
 - => CeO₂ – oxygen storage compounds (Crocker et al., 2008)
- d) Thickness of the storage material particle/layer affects nature and reactivity of adsorbed species (e.g. Ba carbonate vs. carboxylate, cf. Chaugule et al., 2011).

=> Complicated overall picture



(Chaugule et. al., 2010)

Noble metal and NO_x storage sites topology, local transport during the storage

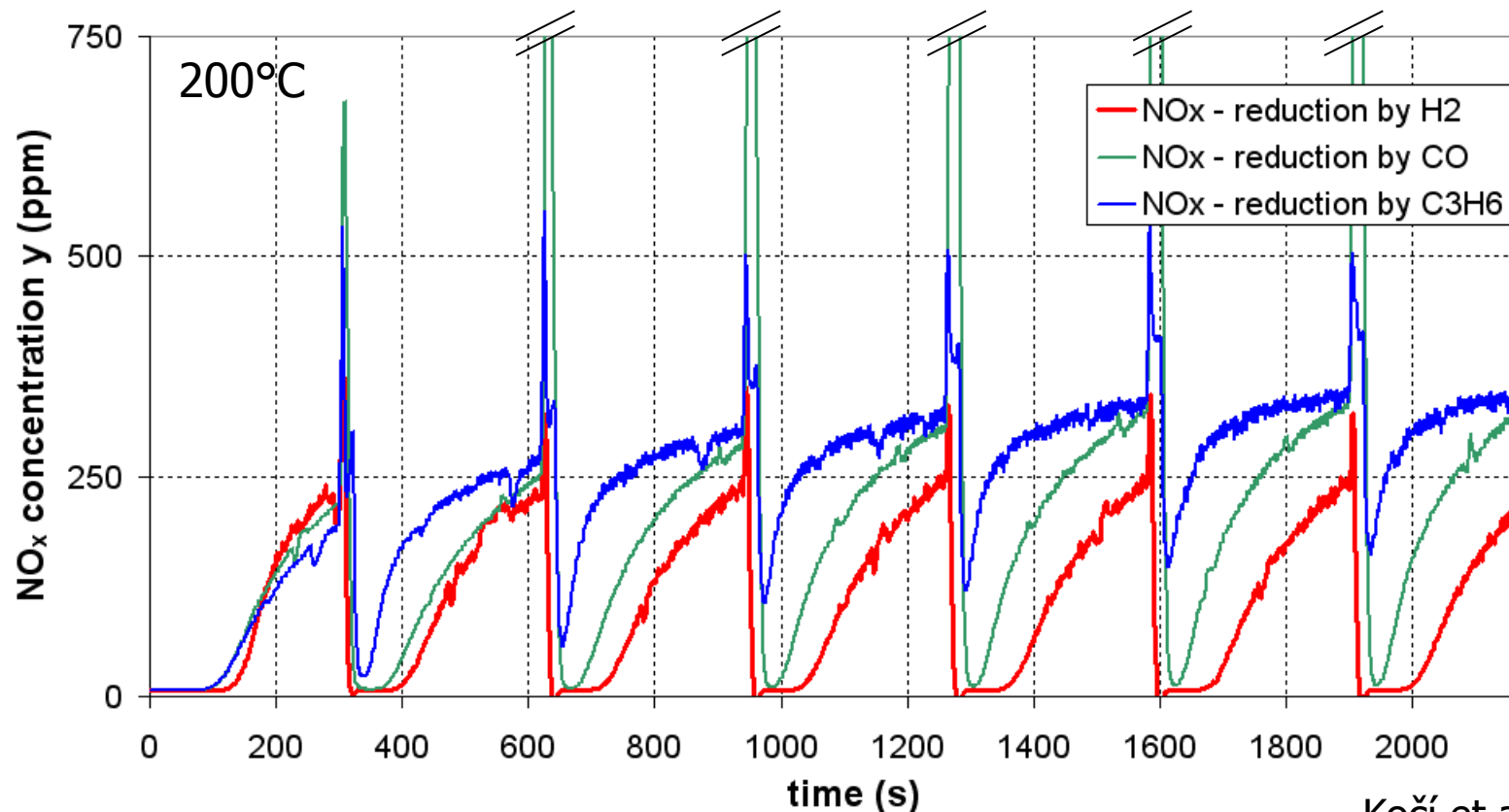
- Local transport models can explain observed dynamics of the NO_x storage:
 - Fast initial storage vs. slow storage when approaching saturation.
 - Slower NO_x release from storage sites distant from Pt, leading to higher NH₃ yield.
- However, surface chemistry mechanisms may lead to similar effects – difficult to split:
 - Fast initial NO_x uptake – nitrites, then slower transformation into nitrates
 - Fast initial regeneration slows down – formation of surface species that inhibit the reaction (-NCO etc.)
- Implementation of the local transport models brings several complications:
 - ⇒ Sizes/contact of active particles are questionable (often there is a wide distribution).
 - ⇒ Local diffusivities are not known exactly → fitted parameters.
 - ⇒ A special sub-model is needed for spatial distribution of stored NO_x in, on, or around the active particles. This additional dimension increases computation time.

Lumping of local transport effects into reaction kinetics

- It is possible to partly lump the local transport effects into the reaction kinetics:
 - Coverage-dependent activation energies (LNT regeneration model by Forzatti et al., 2010)
 - Second order reaction rates with respect to stored NO_x (LNT global kinetic model by Kočí et al., 2009)
 - Two or more kinds of NO_x storage sites according to their reactivity
 - ⇒ "Fast" (easy accessible, Pt contact) and "slow" sites.
 - ⇒ Easier parametrization and computation.
- ⇒ Numbers of sites for each type can be estimated directly from NO_x adsorption experiments (fitted to data) or derived from the more detailed model (Bhatia et al., 2009).

Rich reduction of the stored NO_x

- The stored NO_x can be reduced by H_2 , CO and/or hydrocarbons
 - \Rightarrow The reactivity is $\text{H}_2 > \text{CO} \gg$ hydrocarbons (Kočí et al., 2008, 2009).
 - \Rightarrow CO strongly inhibits the activity of H_2 at low temperatures, therefore in reality it is very difficult to efficiently regenerate the catalyst below 200°C .



Integral NO_x conversion and NH_3 selectivity trends

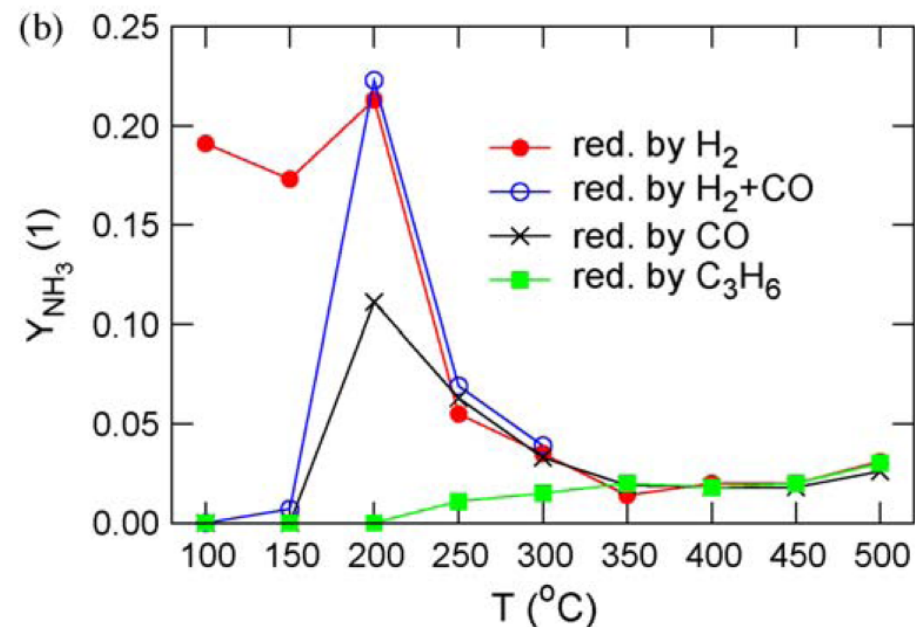
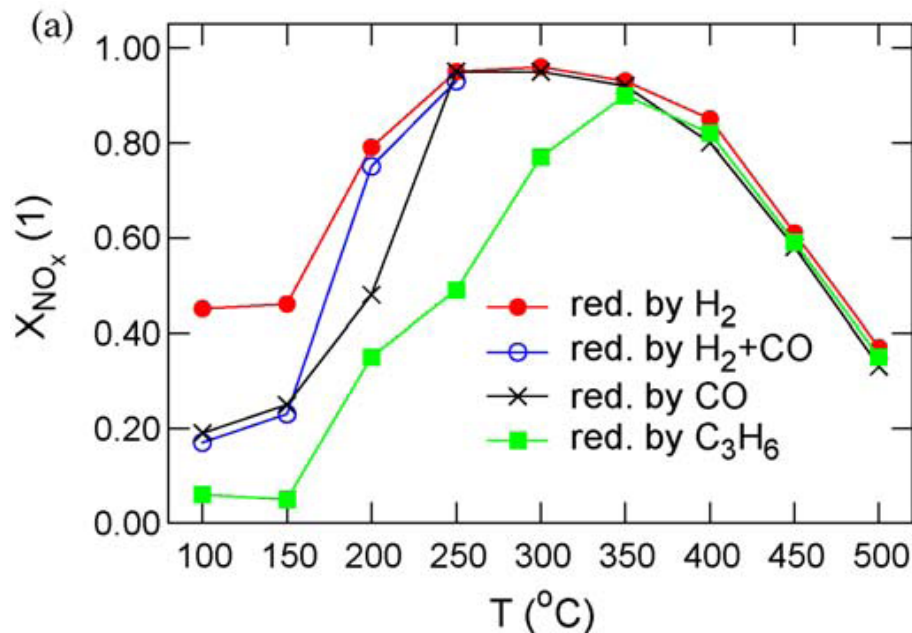
Periodic lean/rich operation 300s/20s

Low temperatures

- NO_x reduction activity $\text{H}_2 > \text{CO} > \text{C}_3\text{H}_6$; **inhibition of H_2 by CO .**
- high NH_3 yield with H_2 , also with CO but not below 200°C (inhibited). No NH_3 with C_3H_6 .

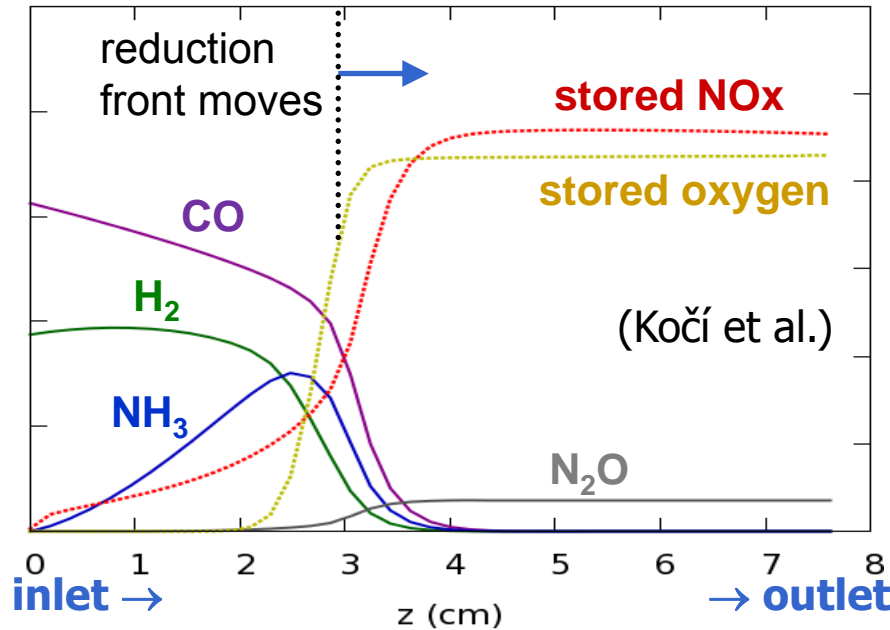
High temperatures

- H_2 , CO and C_3H_6 equivalent; regeneration limited by feed of the reductants.
- low NH_3 yield with all reducing agents because of fast NH_3 oxidation.

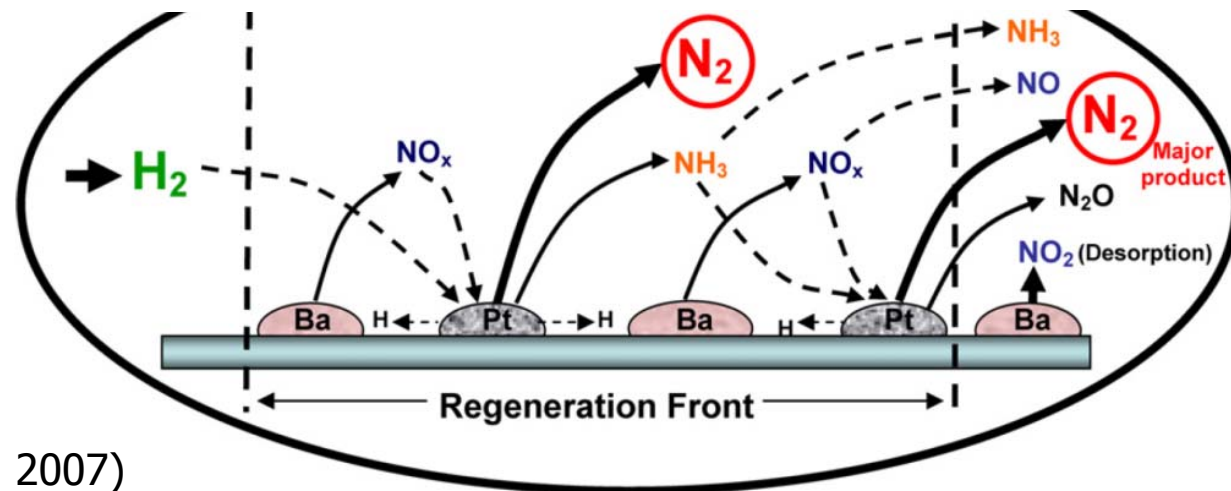


Kočí et al., 2009

Rich reduction of the stored NO_x Moving regeneration front, NH_3 formation and consumption

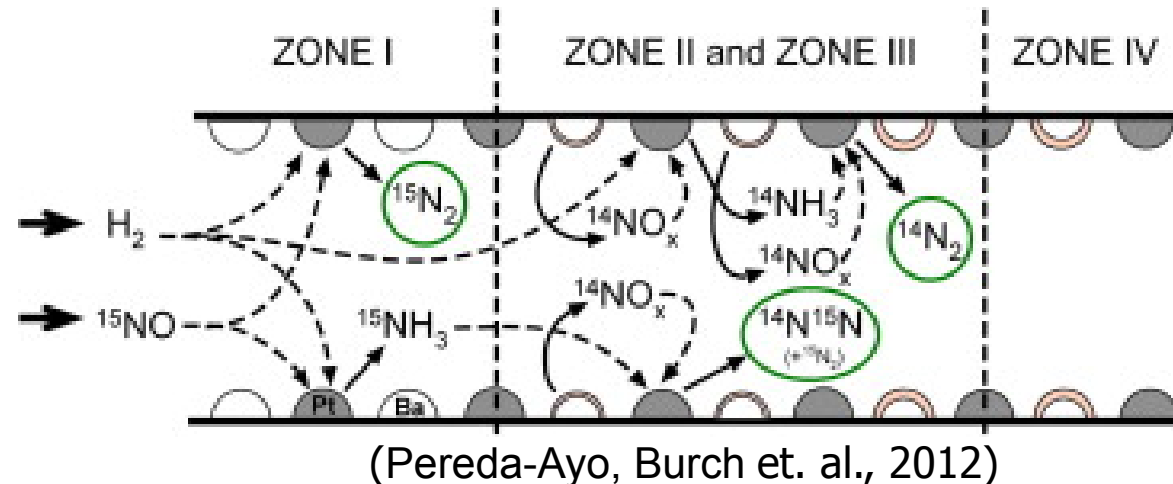


- Large part of the stored NO_x is reduced in the rich zone up to ammonia, and the formed NH_3 is transported downstream where it reacts again with the stored NO_x to N_2 or N_2O
- NH_3 is formed significantly also during the NO_x reduction by CO in the presence of H_2O (water gas shift or isocyanates route)



Rich reduction of the stored NO_x – N_2 formation pathways

- Ammonia formation and re-oxidation pathway is not the unique source of N_2 during the LNT regeneration (though it is the major one under rich conditions).
- Direct N_2 formation during LNT reduction suggested by isotope labeling study:



- The existing global kinetic models (Kočí et al., 2009; Bhatia et al., 2009) and some microkinetic models (Forzatti et al., 2010) consider NH_3 as the unique product of NO_x reduction by H_2 . N_2 formation results from NH_3 re-oxidation by stored O_2 or NO_x .
- Probability of direct N_2 formation is present in some microkinetic models (Lindholm, 2008, Larsson, 2012). However, quantification of the ratio between the two routes is almost impossible from typical LNT regeneration data used for the model calibration.

Rich reduction of the stored NO_x Other important considerations

- Oxygen storage materials are always present in fully formulated commercial LNT.
⇒ The stored oxygen consumes a considerable amount of reducing agents (up to 1/2), affects breakthrough of CO, H₂, HC and NH₃. (Kočí et al., 2008, Choi et al., 2009).
- At low-intermediate temperatures (<300°C, for HC up to 350°C), the regeneration is kinetically limited, i.e., the composition of rich mixture (CO, H₂, HC) matters:
 - different NO_x conversion,
 - different NO_x reduction selectivity (NO/N₂O/N₂/NH₃).⇒ Limited applicability of single-reductant models (e.g. H₂ only) in real operation.
- The stored NO_x (surface nitrites and nitrates) can be de-stabilized and desorbed by:
 - Just removing oxygen from gas phase
 - Increasing temperature (exothermic regeneration)⇒ NO_x desorption peak.
- The stored NO_x does not need to be desorbed to gas phase before the reduction – direct spill-over from storage to redox sites exists.

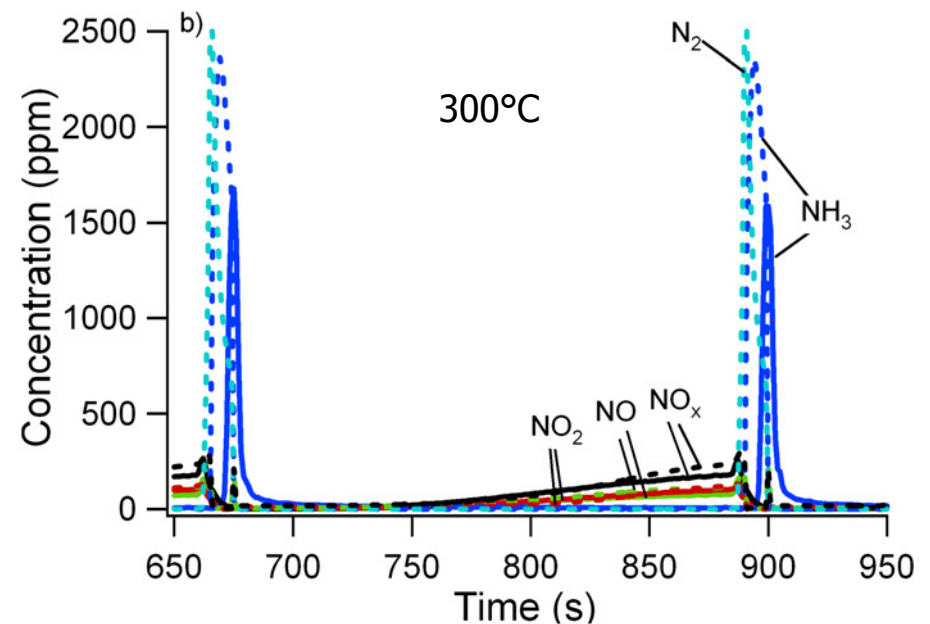
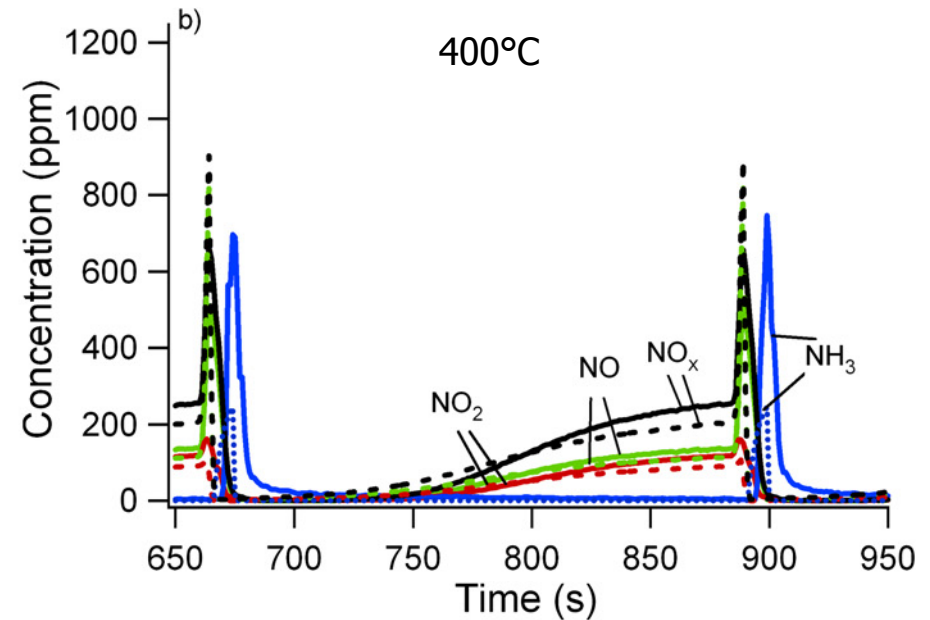
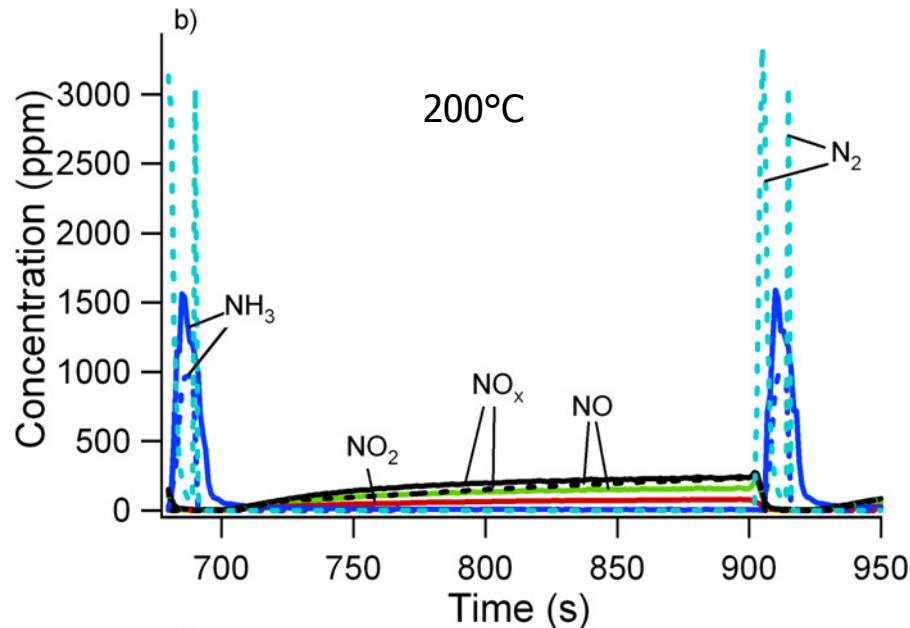
LNT microkinetic models

- Microkinetics:
 - ⇒ Good for mechanistic considerations, testing and identification of reaction mechanisms and mutual relations between adsorbed species
 - ⇒ Large number of reaction intermediates on the surface, Langmuir-Hinshelwood and Eley-Rideal reaction pathways.
 - ⇒ Too complex with realistic exhaust gas compositions (CO, H₂, HCs), or simplifications must be accepted that compromise the idea of "pure" microkinetics for LNT.
 - ⇒ Some surface species at very low concentrations may determine the rate => usually more stiff than global kinetics.
 - ⇒ Real NO_x storage catalyst contains several types of NO_x storage sites, covered by nitrites and nitrates – a large number of just different kinds of adsorbed NO_x species. If each can interact with all reducing agents, the number of reaction steps is high.
 - ⇒ E.g. Olsson et al., 2001; Lindholm et al., 2008; Larson et al., 2012

LNT microkinetic models

Lindholm et al. (2008):

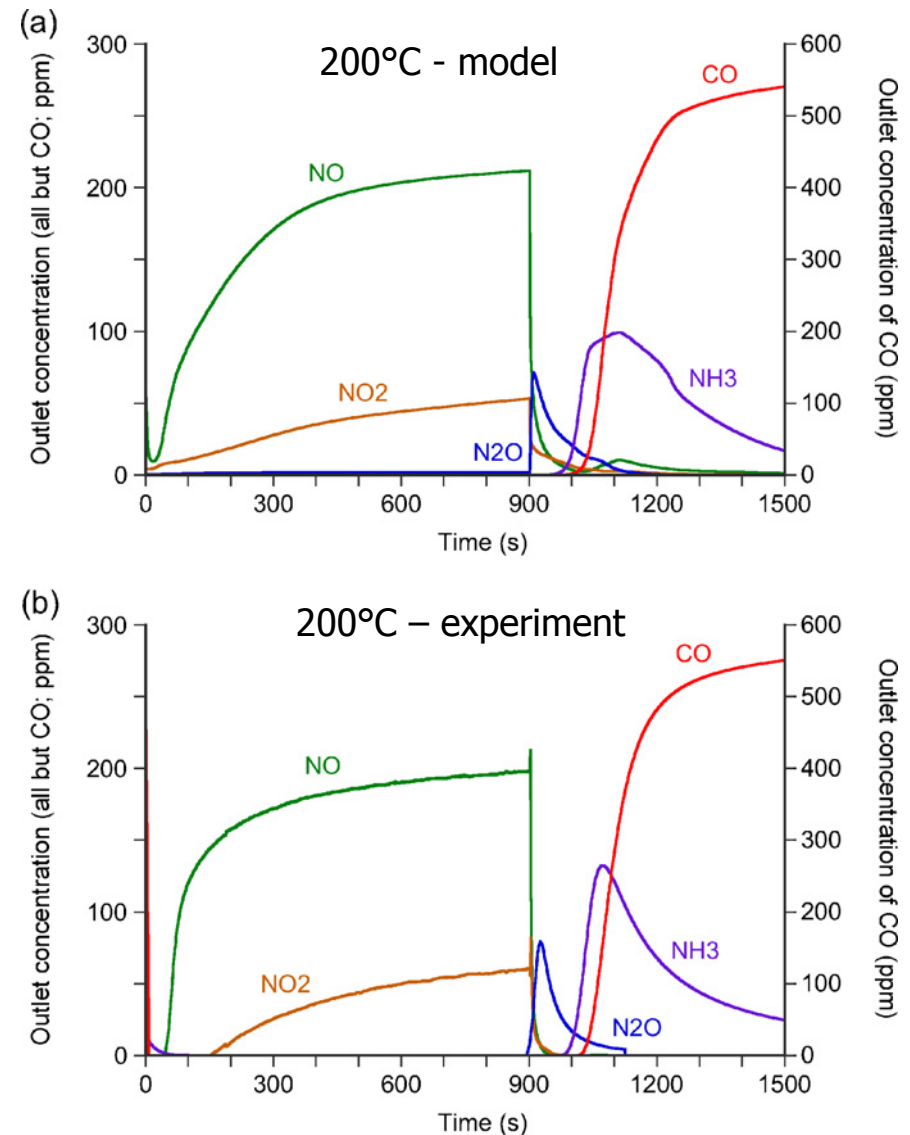
- Detailed NO_x adsorption (Olsson, 2001)
- 41 reaction steps, 6 adsorbed species on Pt, 5 kinds of stored NO_x on two different sites
- Several rate coefficients fixed from DFT etc
- H₂ as primary reductant, NH₃ as a key intermediate, N₂O not considered
- Pt/Ba/Al₂O₃, no oxygen storage capacity
- Basic trends captured well, but too early and high NH₃ peak at 300°C.



LNT microkinetic models

Larson et al. (2012):

- Complex model with reversibility and global thermodynamic constraints considered for all reactions.
- 44 reaction steps, 13 adsorbed species on Pt sites, 5 kinds of stored NO_x on one site.
- Still not elementary steps.
- Many spillover reactions between the sites.
- Parameters optimized.
- Reaction kinetics embedded in isothermal monolith model.
- Fully formulated LNT with oxygen storage.
- Reduction by mixture of CO and H_2 .
- N_2O formation considered.
- Good results for both slow temperature ramps and long cycles at 200-400°C with low reductant concentration.
- Discrepancy reported for short cycles with high reductant concentration – parameters readjustment needed.



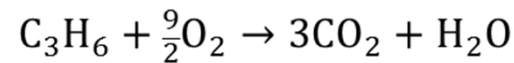
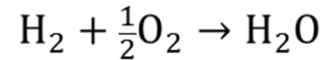
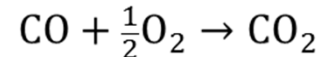
LNT global kinetics

- Global kinetics:
 - ⇒ Only key surface species that accumulate to a significant extent are considered explicitly (typically: stored oxygen and 2 types of stored NO_x – fast, slow).
 - ⇒ Other reaction intermediates are considered in pseudo-steady state, i.e., the rate laws are formulated in dependence on local gas concentrations.
 - ⇒ Lower number of reaction steps and components, smaller and less stiff system, faster numerical solution
 - ⇒ Higher freedom in describing mutual inhibition effects and non-idealities.
 - ⇒ The extent of simplification must be carefully chosen to keep the balance between limited number of reaction steps and ability to capture important features during transient operation.
 - ⇒ E.g. Kočí et al., 2004, 2008, 2009; Olsson et al., 2005; Cao et al., 2008; Bhatia et al., 2009.

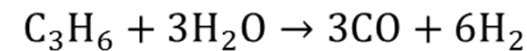
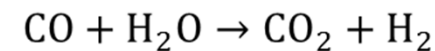


Global model reactions – oxidation/reduction over NM sites

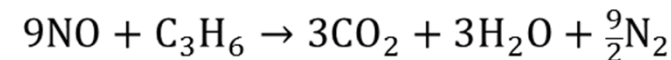
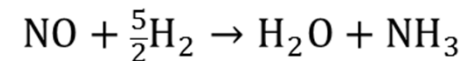
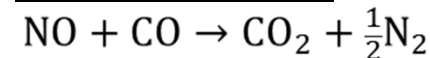
Reductant oxidation



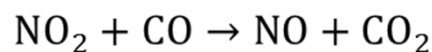
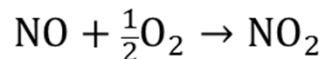
Water gas shift and steam reforming



NO reduction



NO/NO₂ transformation



$$G_1 = (1 + K_{a,1}Y_{\text{CO}} + K_{a,2}Y_{\text{C}_3\text{H}_6})^2 \cdot (K_{a,3}Y_{\text{CO}}^2 Y_{\text{C}_3\text{H}_6}^2) \cdot (1 + K_{a,4}Y_{\text{NO}_x}^{0.7}) T^s$$

$$G_2 = 1 + K_{a,5}Y_{\text{O}_2}$$

(Kočí et al., 2009)

$$R_1 = k_1 \Psi_{\text{cap,Pt}} Y_{\text{CO}} Y_{\text{O}_2} \frac{1}{G_1}$$

$$R_2 = k_2 \Psi_{\text{cap,Pt}} Y_{\text{H}_2} Y_{\text{O}_2} \frac{1}{G_1}$$

$$R_3 = k_3 \Psi_{\text{cap,Pt}} Y_{\text{C}_3\text{H}_6} Y_{\text{O}_2} \frac{1}{G_1}$$

$$R_4 = k_4 \Psi_{\text{cap,Pt}} \left(Y_{\text{CO}} Y_{\text{H}_2\text{O}} - \frac{Y_{\text{CO}_2} Y_{\text{H}_2}}{K_{y,4}^{\text{eq}}} \right)$$

$$R_5 = k_5 \Psi_{\text{cap,Pt}} \left(Y_{\text{C}_3\text{H}_6} Y_{\text{H}_2\text{O}} - \frac{Y_{\text{CO}}^3 Y_{\text{H}_2}^6}{K_{y,5}^{\text{eq}} Y_{\text{H}_2\text{O}}^2} \right)$$

$$R_6 = k_6 \Psi_{\text{cap,Pt}} Y_{\text{CO}} Y_{\text{NO}}^{0.5} \frac{1}{G_2} \frac{1}{G_1}$$

$$R_7 = k_7 \Psi_{\text{cap,Pt}} Y_{\text{H}_2} Y_{\text{NO}}^{0.5} \frac{1}{G_2} \frac{1}{G_1}$$

$$R_8 = k_8 \Psi_{\text{cap,Pt}} Y_{\text{C}_3\text{H}_6} Y_{\text{NO}}^{0.5} \frac{1}{G_2} \frac{1}{G_1}$$

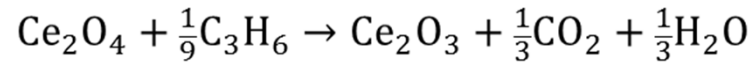
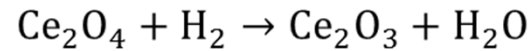
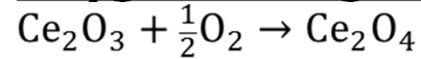
$$R_9 = k_9 \Psi_{\text{cap,Pt}} \left(Y_{\text{NO}} Y_{\text{O}_2}^{0.5} - \frac{Y_{\text{NO}_2}}{K_{y,9}^{\text{eq}}} \right) \frac{1}{G_1}$$

$$R_{10} = k_{10} \Psi_{\text{cap,Pt}} Y_{\text{NO}_2} Y_{\text{CO}} \frac{1}{G_{\text{NO}_2, \text{red}}}$$

$$R_{11} = k_{11} \Psi_{\text{cap,Pt}} Y_{\text{NO}_2} Y_{\text{C}_3\text{H}_6} \frac{1}{G_{\text{NO}_2, \text{red}}}$$

Global model reactions – storage and release

Oxygen storage & reduction



(Kočí et al., 2009, Chatterjee et al., 2010)

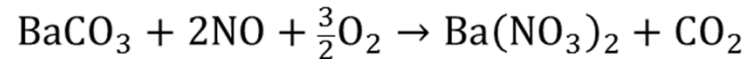
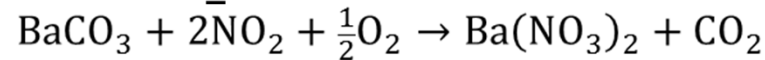
$$R_{12} = k_{12} \Psi_{\text{cap,CeO}_2} y_{\text{O}_2} (\psi_{\text{O}_2}^{\text{eq}} - \psi_{\text{O}_2})$$

$$R_{13} = k_{13} \Psi_{\text{cap,CeO}_2} y_{\text{CO}} \psi_{\text{O}_2}$$

$$R_{14} = k_{14} \Psi_{\text{cap,CeO}_2} y_{\text{H}_2} \psi_{\text{O}_2}$$

$$R_{15} = k_{15} \Psi_{\text{cap,CeO}_2} y_{\text{C}_3\text{H}_6} \psi_{\text{O}_2}$$

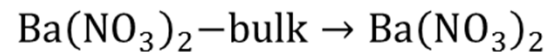
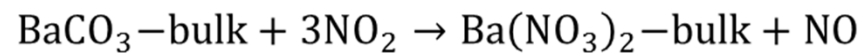
Fast NO_x storage (Ba sites in proximity of Pt)



$$R_{16} = k_{16} \Psi_{\text{cap,Ba}_A} y_{\text{NO}_2} (\psi_{\text{NO}_{x,A}}^{\text{eq}} - \psi_{\text{NO}_{x,A}})^2$$

$$R_{17} = k_{17} \Psi_{\text{cap,Ba}_A} y_{\text{NO}} (\psi_{\text{NO}_{x,A}}^{\text{eq}} - \psi_{\text{NO}_{x,A}})^2$$

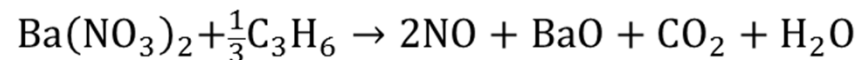
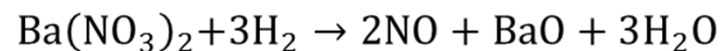
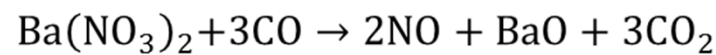
Slow NO_x storage (bulk Ba sites)



$$R_{29} = k_{29} \Psi_{\text{cap,Ba}_B} y_{\text{NO}_2} (\psi_{\text{NO}_{x,B}}^{\text{eq}} - \psi_{\text{NO}_{x,B}})^2$$

$$R_{30} = k_{30} \Psi_{\text{cap,Ba}_B} y_{\text{NO}_2} (\psi_{\text{NO}_{x,B}} - \psi_{\text{NO}_{x,A}})$$

Desorption of stored NO_x

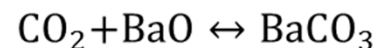


$$R_{22} = k_{22} \Psi_{\text{cap,Ba}_A} y_{\text{CO}} \psi_{\text{NO}_{x,A}}^2 \frac{1}{G_4}$$

$$R_{23} = k_{23} \Psi_{\text{cap,Ba}_A} y_{\text{H}_2} \psi_{\text{NO}_{x,A}}^2 \frac{1}{G_4}$$

$$R_{24} = k_{24} \Psi_{\text{cap,Ba}_A} y_{\text{C}_3\text{H}_6} \psi_{\text{NO}_{x,A}}^2 \frac{1}{G_4}$$

CO₂ adsorption on NO_x storage sites



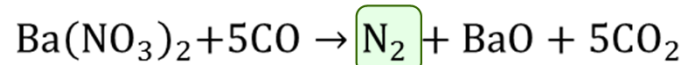
$$G_4 = (1 + 0.1K_{a,6}y_{\text{O}_2})(1 + K_{a,7}y_{\text{NO}_x})$$

$$R_{31} = \sum_{j=18}^{25} R_j$$

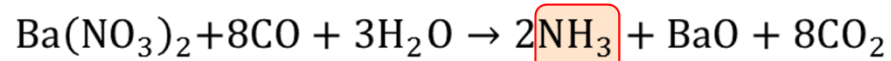
Global model reactions – reduction of nitrates

“Classical” approach with NH₃ intermediate and N₂ product

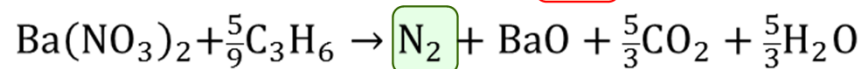
Direct reduction of stored NO_x (Ba sites in proximity of Pt) (Kočí et al., 2009)



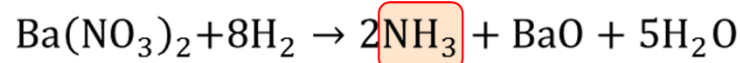
$$R_{18} = k_{18} \Psi_{\text{cap,Ba}_A} y_{\text{CO}} \psi_{\text{NO}_{x,A}}^2 \frac{1}{G_3}$$



$$R_{19} = k_{19} \Psi_{\text{cap,Ba}_A} y_{\text{CO}} \psi_{\text{NO}_{x,A}}^2 \frac{1}{G_3} \frac{1}{G_5}$$

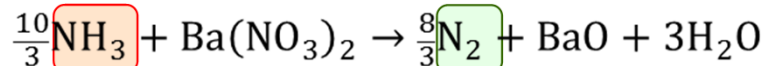


$$R_{21} = k_{21} \Psi_{\text{cap,Ba}_A} y_{\text{C}_3\text{H}_6} \psi_{\text{NO}_{x,A}}^2 \frac{1}{G_3}$$

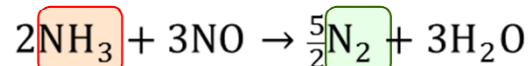


$$R_{20} = k_{20} \Psi_{\text{cap,Ba}_A} y_{\text{H}_2} \psi_{\text{NO}_{x,A}}^2 \frac{1}{G_3} \frac{1}{G_5}$$

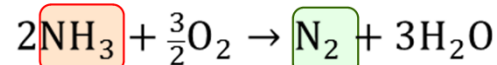
NH₃ oxidation reactions – N₂ formation



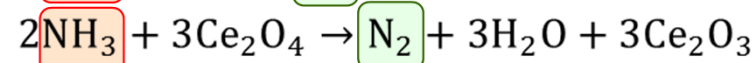
$$R_{25} = k_{25} \Psi_{\text{cap,Ba}_A} y_{\text{NH}_3} \psi_{\text{NO}_{x,A}}^2$$



$$R_{26} = k_{26} \Psi_{\text{cap,Pt}} y_{\text{NH}_3} y_{\text{NO}}^{0.5}$$



$$R_{27} = k_{27} \Psi_{\text{cap,Pt}} y_{\text{NH}_3} y_{\text{O}_2}$$



$$R_{28} = k_{28} \Psi_{\text{cap,CeO}_2} y_{\text{NH}_3} \psi_{\text{CeO}_2}$$

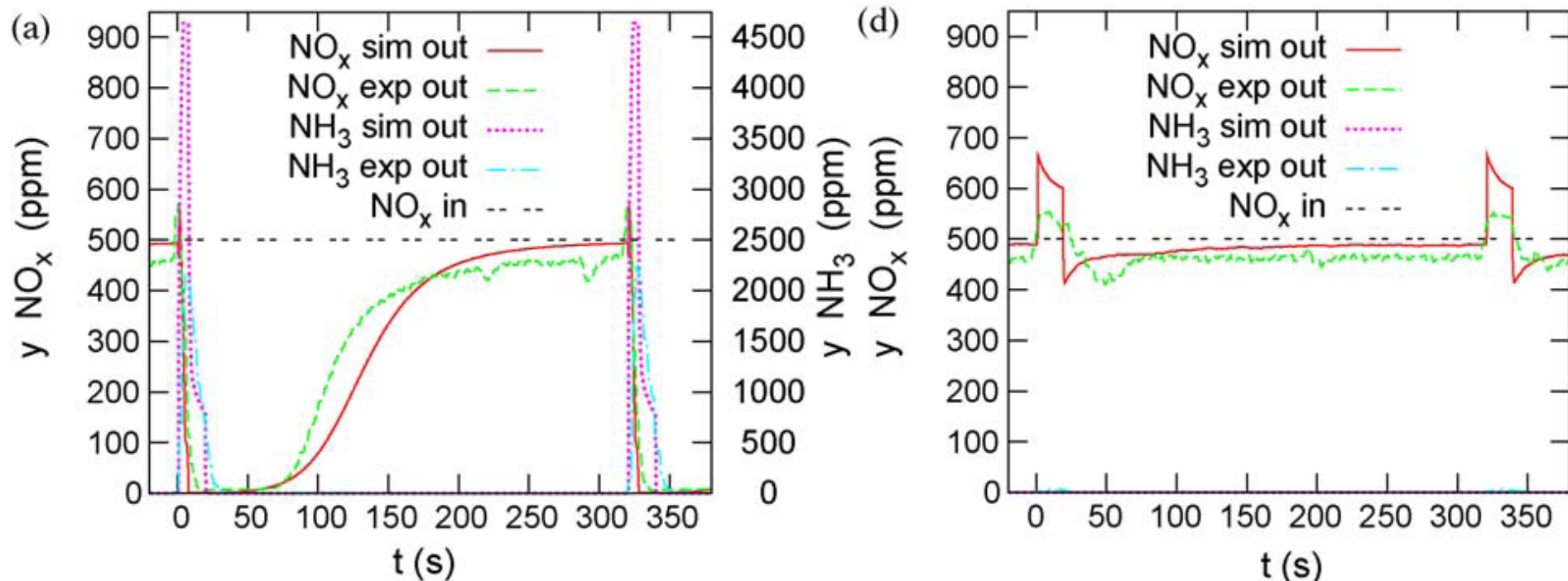
$$G_3 = 1 + K_{a,6} y_{\text{O}_2} \quad G_5 = 1 + K_{a,8} y_{\text{CO}}$$

Periodic lean/rich operation – 150°C

Low temperature – comparison of the reduction by H_2 and C_3H_6

Reduction by C_3H_6 practically does not take place.

NO_x reduction by pure H_2 is quite effective and a large NH_3 peak is observed shortly after the start of the regeneration, NH_3 consumption reactions are not very active yet.

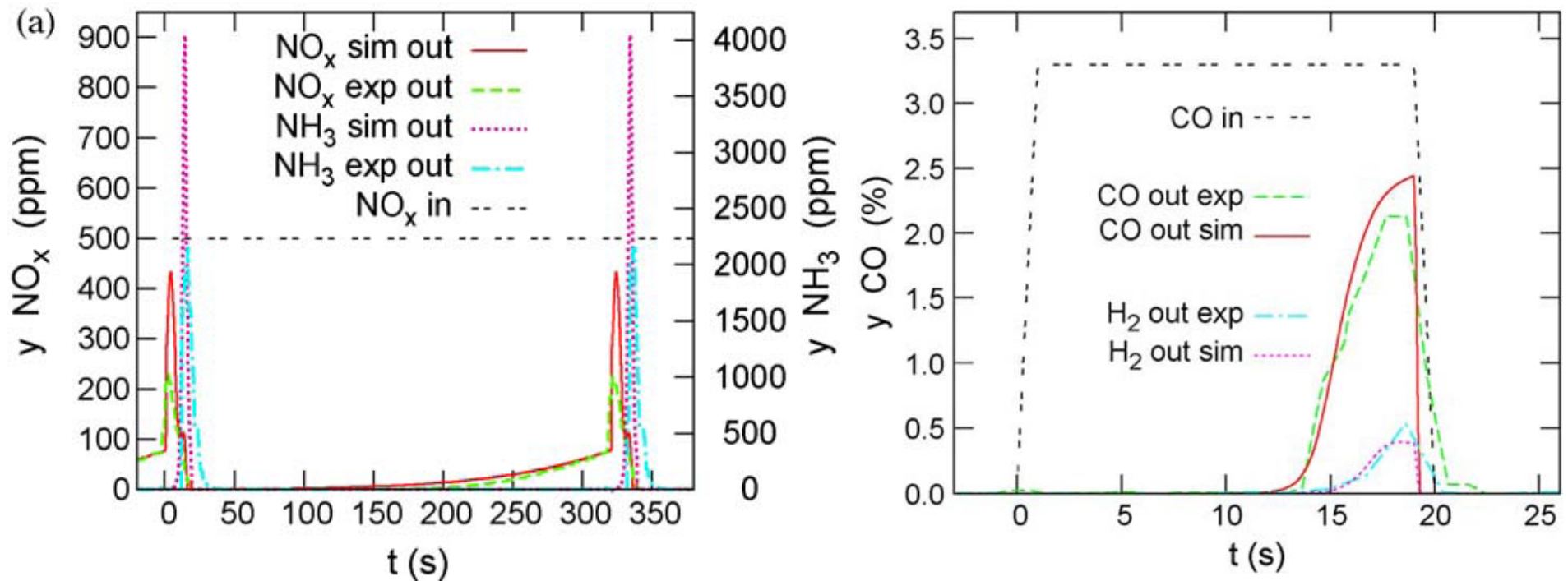


Periodic lean/rich operation – 250°C

Intermediate temperature – the reduction by CO.

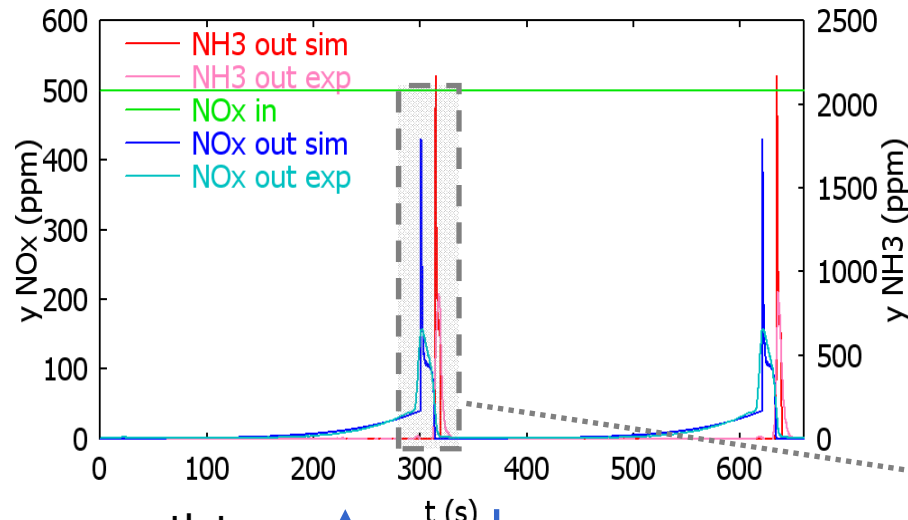
NH₃ formation in presence of H₂O, but the NH₃ peak is observed with a substantial delay after the start of the regeneration due to internal NH₃ re-oxidation.

⇒ The breakthrough time is determined by actual amount of stored oxygen and NO_x

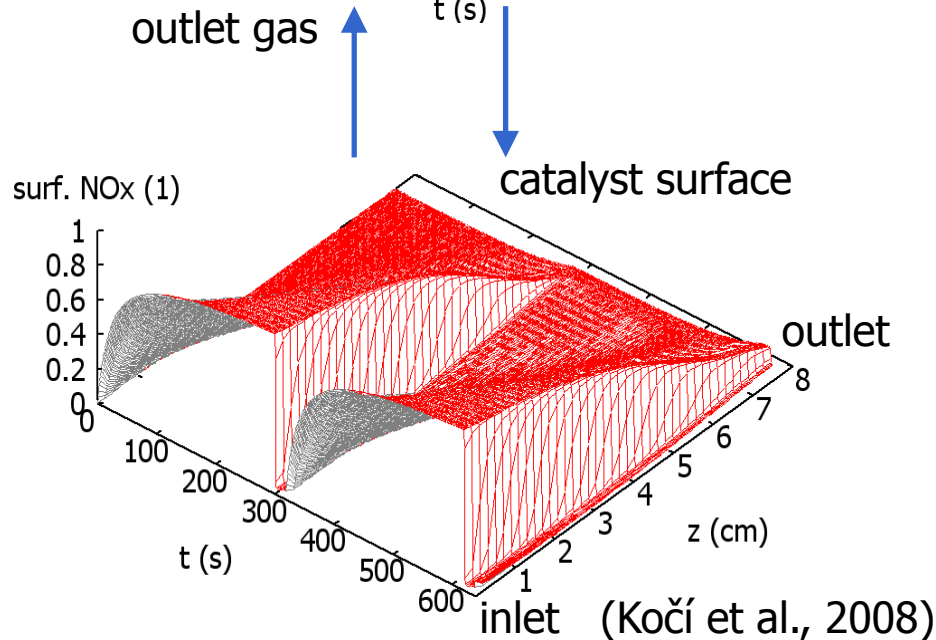
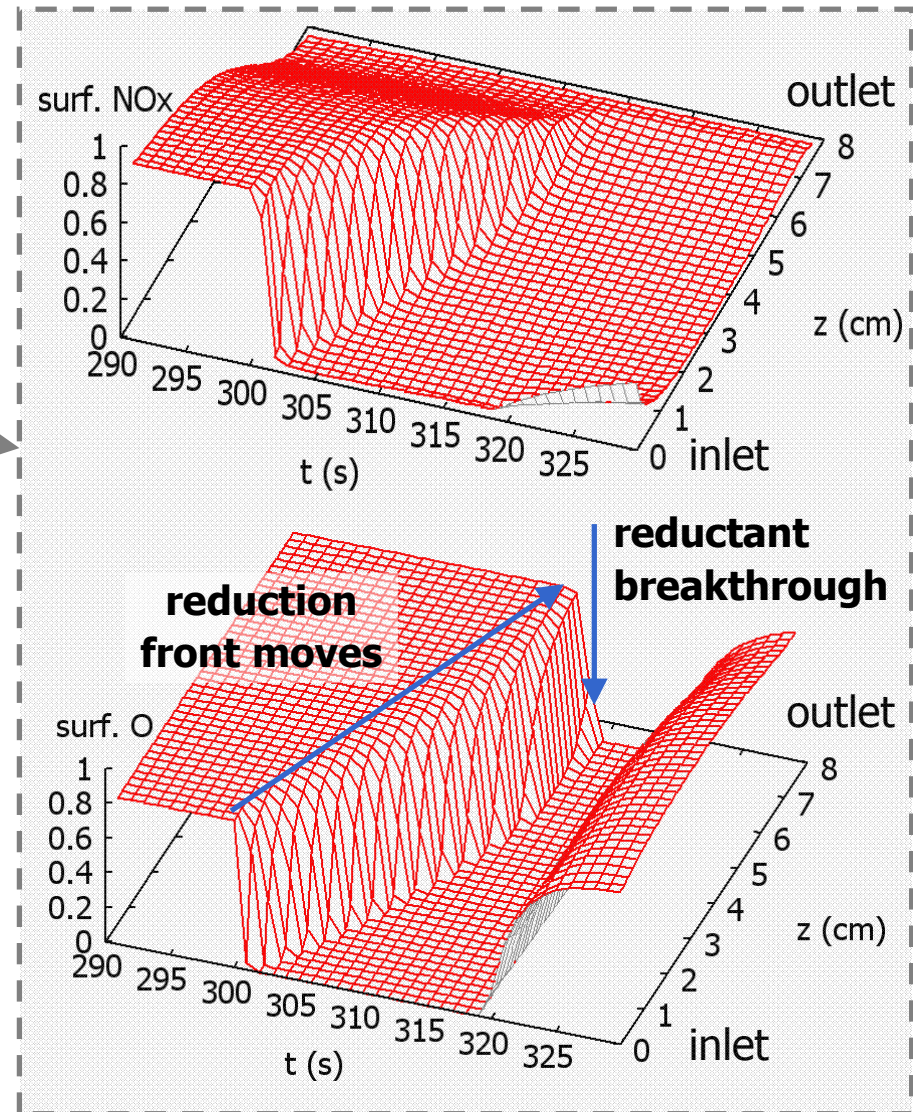


Kočí et al., 2009

Surface regeneration during the rich phase – moving fronts

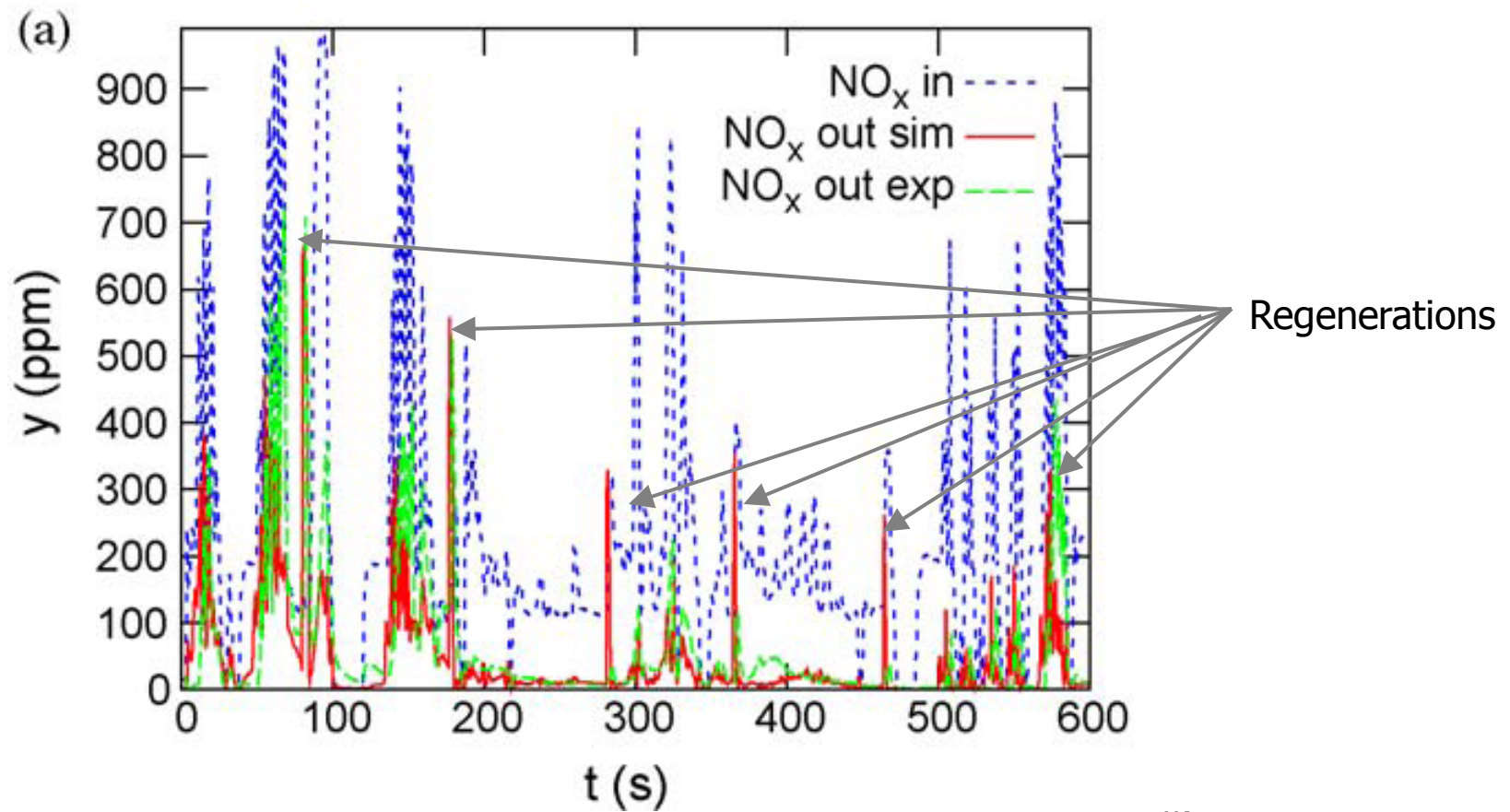


Detail of stored NO_x and O during regen



Model validation – test driving cycle SFTP US06

Dynamic evolution of NO_x concentrations at the converter inlet and outlet



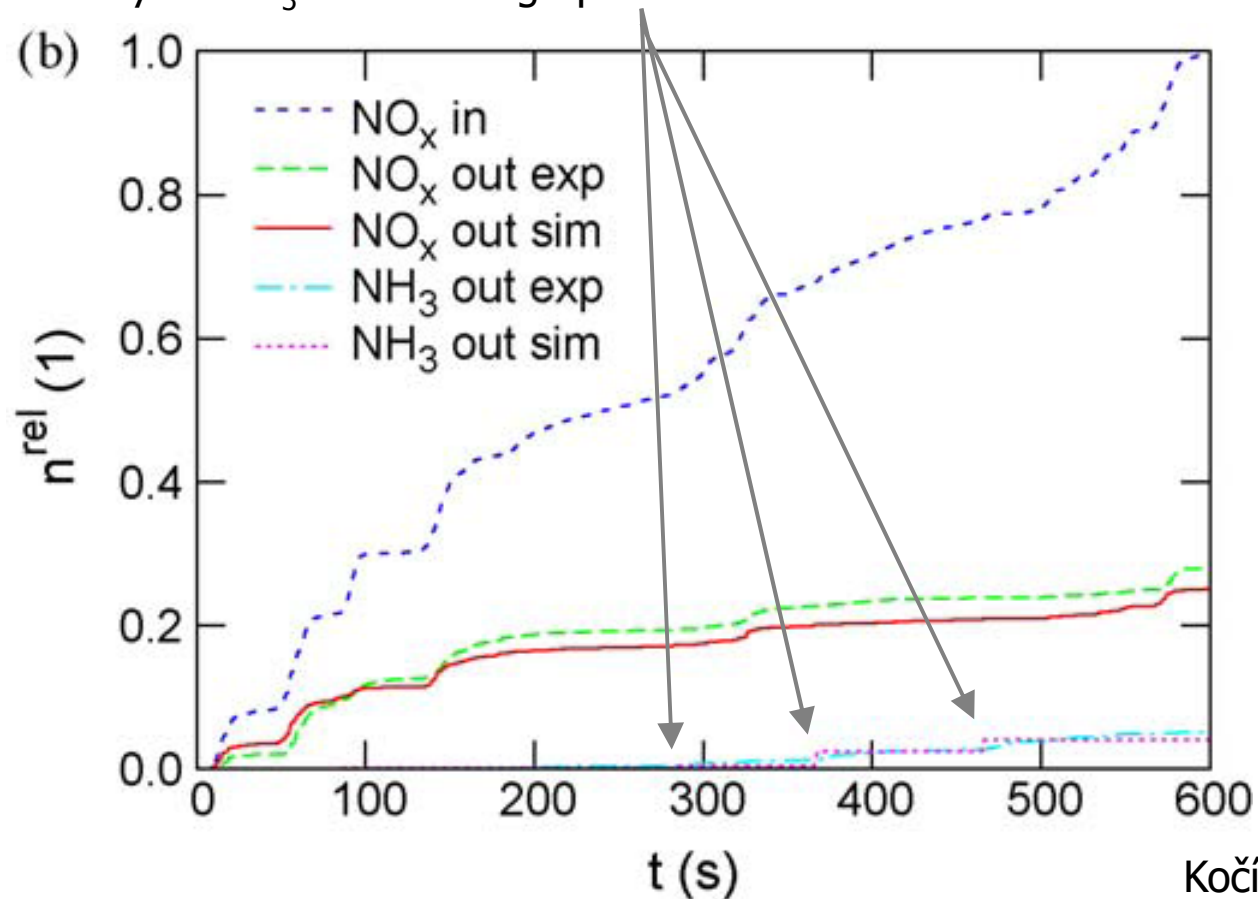
Kočí et al., 2009

Model validation – test driving cycle

SFTP US06

Cumulative (integrated) NO_x and NH_3 emissions at the converter inlet and outlet

Each increase in cumulative NH_3 emissions corresponds to the catalyst regeneration accompanied by an NH_3 breakthrough peak.



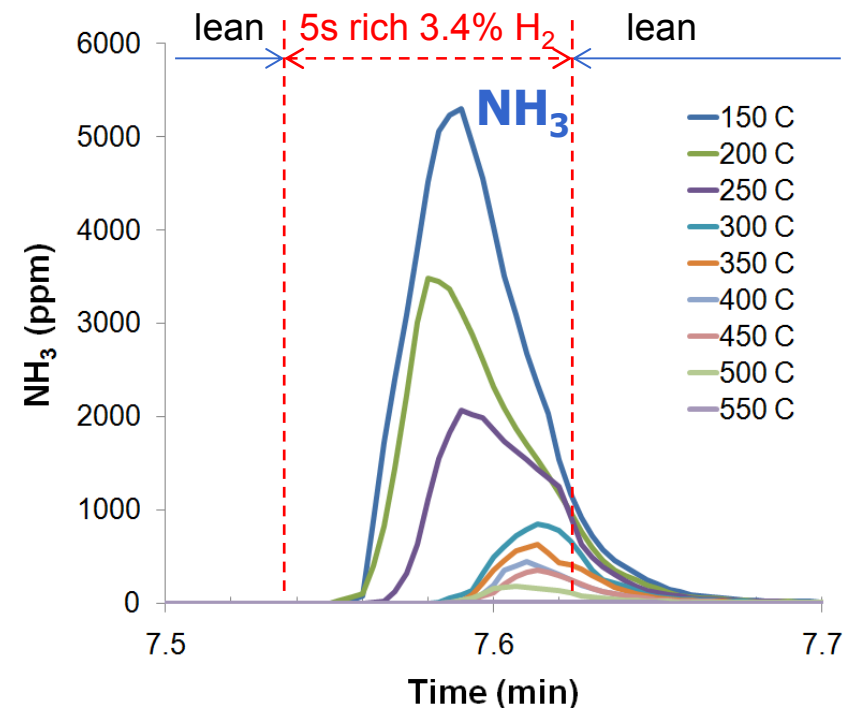
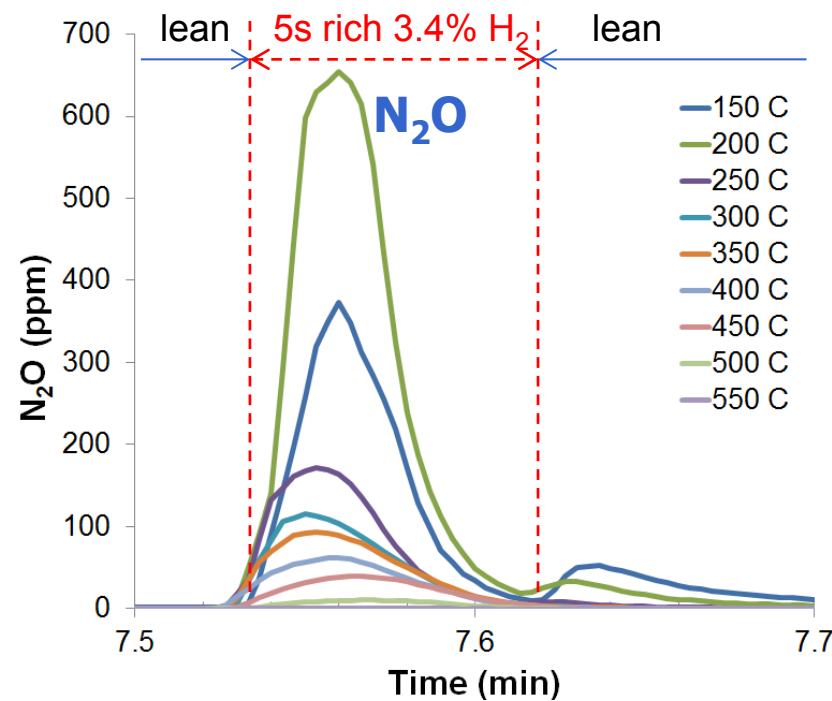
Kočí et al., 2009

Current topic in automotive exhaust gas aftertreatment: N₂O Emissions

- N₂O is an **undesired by-product** of catalytic NO_x reduction in exhaust gas aftertreatment systems particularly of lean-burn engines.
 - **DOC** – non-selective HC-SCR at lower-intermediate T
 - **NH₃-SCR** – too high NO₂/NO_x ratio, NH₄NO₃ decomposition, NH₃ oxidation
 - **NH₃ slip** catalyst (=ASC) – non-selective NH₃ oxidation
 - **LNT** (=NSRC) regeneration
- N₂O in low concentrations pose **no health risk**. Global average in atmosphere ~ 0.3 ppm.
- N₂O is a strong **greenhouse gas** (global warming potential ~300 x higher than CO₂). Mean N₂O tailpipe concentrations are typically 10³-10⁵ lower than those of CO₂, therefore overall GHG contribution of N₂O in automotive exhaust gas can vary from 0.1 % up to several %.
- **Natural sources** (biological processes in soil and water) ~ 60% of total N₂O emissions. The main human-related source of N₂O is **agricultural soil management** (fertilizers), **adipic and nitric acid production**, and **combustion of fossil fuels**.
- Mobile N₂O emissions have **been unregulated**, but the limits are expected in near future (CARB LEVIII regulations, Euro VI+?)

N₂O Sources in LNT

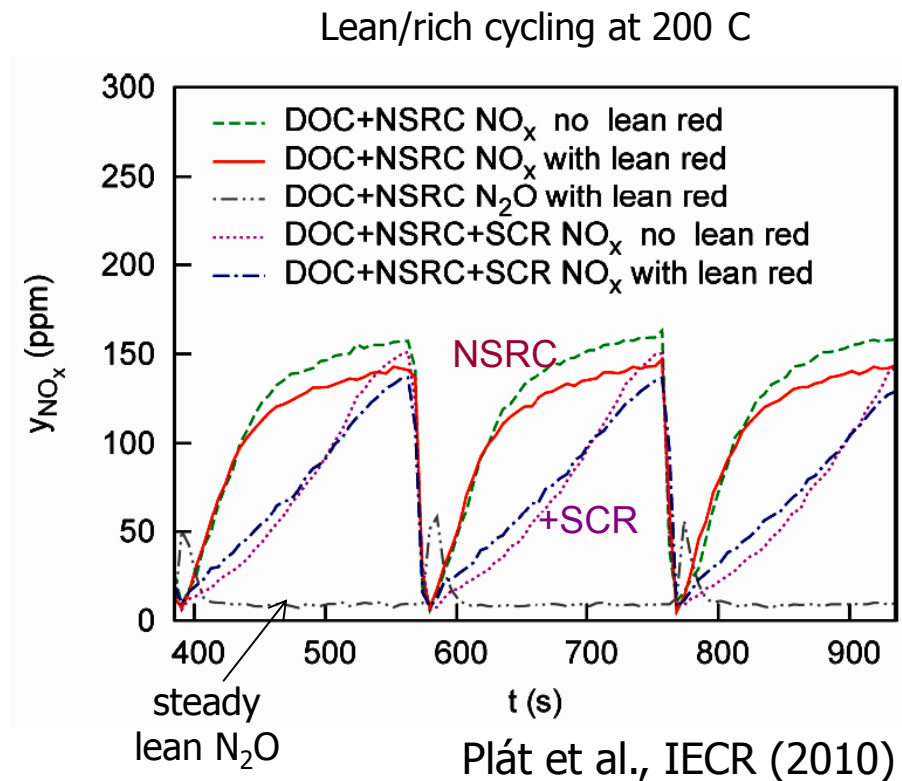
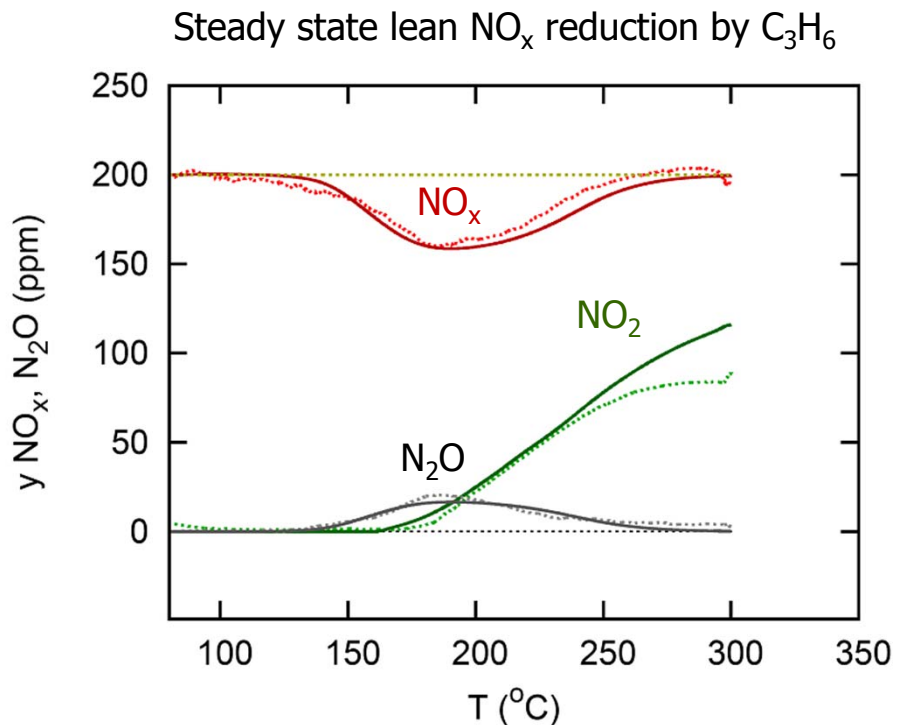
1. Non-selective HC-SCR during lean phase at lower-intermediate temperatures in presence of hydrocarbons – steady process. Takes place already in upstream TWC/DOC (if present).
2. LNT regeneration – primary N₂O peak appears after the switch to rich conditions.
3. LNT regeneration – secondary (smaller) N₂O peak at the switch back to lean conditions



Pihl et al. (ORNL), CLEERS LNT data

N₂O Source 1: Lean NO_x Reduction by Hydrocarbons

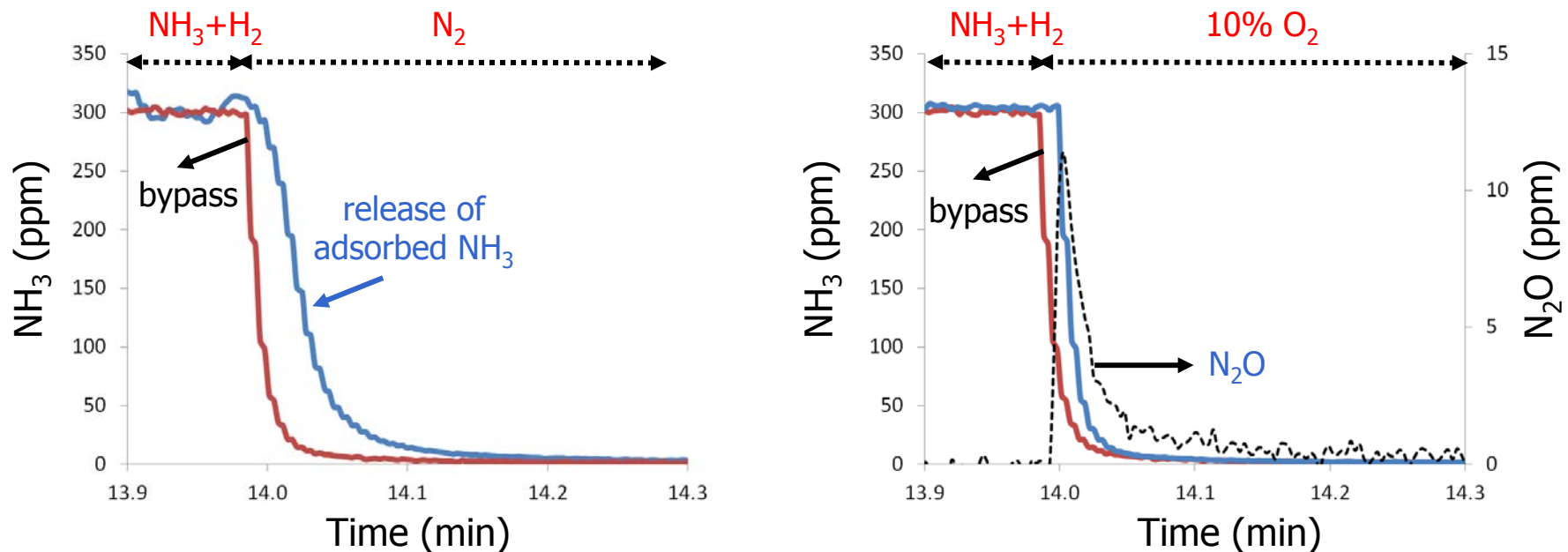
- Lean NO_x reduction by HC takes place in a lower-intermediate temperature window.
- N₂O selectivity very high (0.5–1.0), independent on temperature.
- Takes place in all PGM-based catalysts (TWC, DOC, LNT, CDPF) under lean conditions.
- Steady process – relatively low N₂O concentration but sums up over a long time.
- Occurs primarily in the upstream TWC/DOC (if present).



N₂O Source 2: Oxidation of Adsorbed NH₃ at Transition Back from Rich to Lean Conditions

Several contributions:

- Oxidation of desorbing NH₃ by oxygen to N₂O (non-selective oxidation).
- Decomposition of NH₄NO₃ formed during regeneration.
- Oxidation of NO_x+HC reduction intermediates remaining on the surface (e.g., R-CNO).



Pihl et al. (ORNL), CLEERS LNT data

- NO_x formation also possible (usually invisible at outlet due to re-storage)

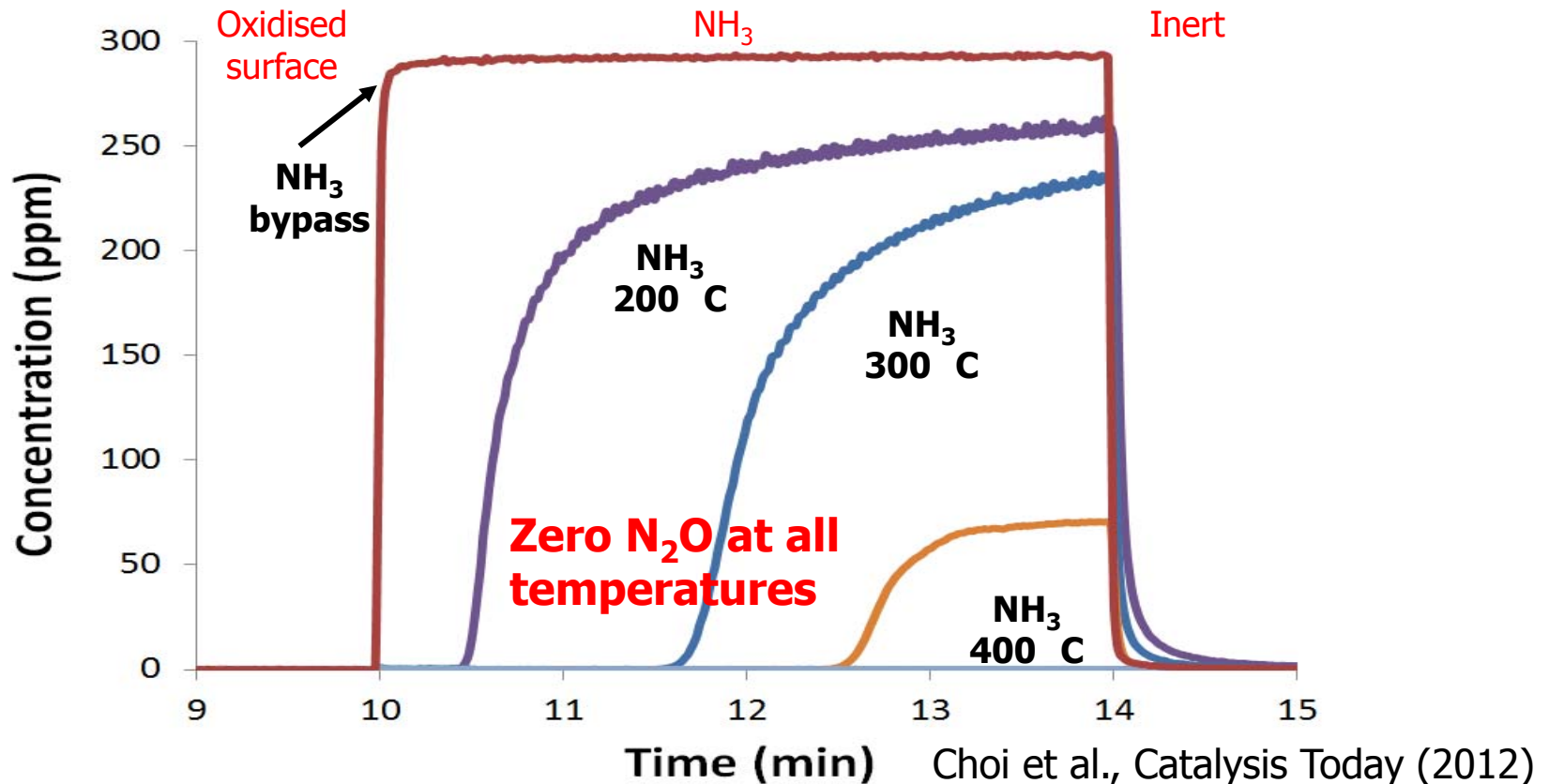
N₂O Source 3: Main N₂O Peak During the Rich Phase Identification of the mechanism...

Several candidate reactions:

- Non-selective NH₃ re-oxidation – poor selectivity of PGM catalysts in NH₃ oxidation is known. There are two main species for NH₃ to react with:
 - Stored oxygen
 - Stored NO_x⇒ The most straightforward extension of the existing global kinetic model.
- “Direct” formation of N₂O during reduction of stored NO_x by primary reductants (H₂, CO and/or HC)
 - Most of the stored NO_x are reduced under locally rich conditions (leading mainly to NH₃), but at the head of the reducing front the reductants initially reach oxidized sites surrounded by stored NO_x – local formation of N₂O possible.

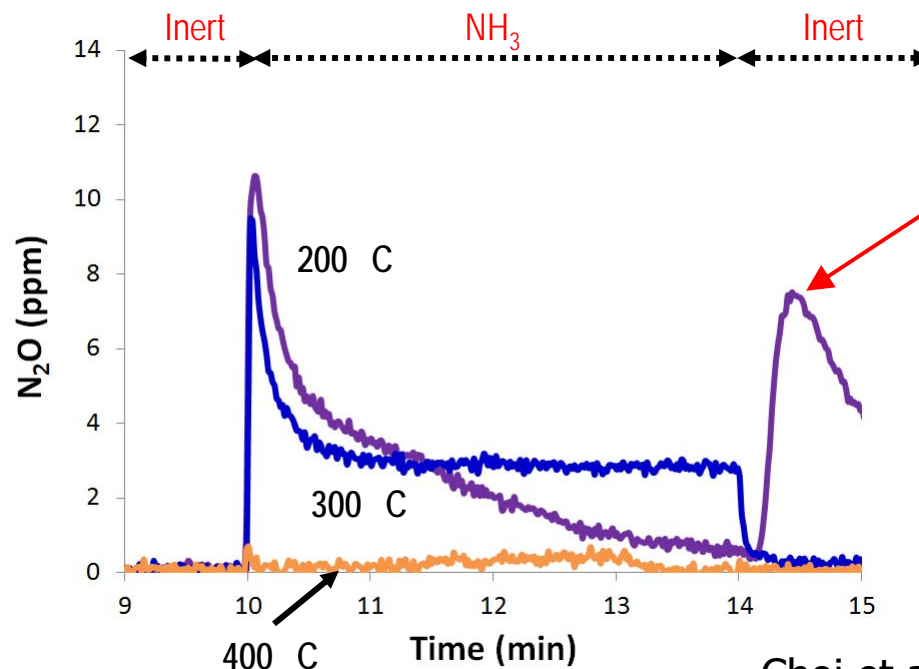
N₂O Source 3: Main N₂O Peak During the Rich Phase Checking NH₃ + stored oxygen

- Pre-oxidised surface (followed by inert purge), then NH₃ introduced.
- The reaction with stored oxygen is very rapid \Rightarrow plug-like behaviour
- Contrary to steady-state NH₃ oxidation, no N₂O is detected. NH₃ decomposition at high T.
 \Rightarrow This reaction does not contribute to N₂O formation.



N₂O Source 3: Main N₂O Peak During the Rich Phase Checking NH₃ + stored NO_x

- Nitrated surface (NO_x + O₂ storage), then inert purge, then NH₃ introduced (no NO_x fed during reduction)
 - N₂O is formed all the time before NH₃ breakthrough.
- ⇒ This reaction definitely contribute to N₂O formation.

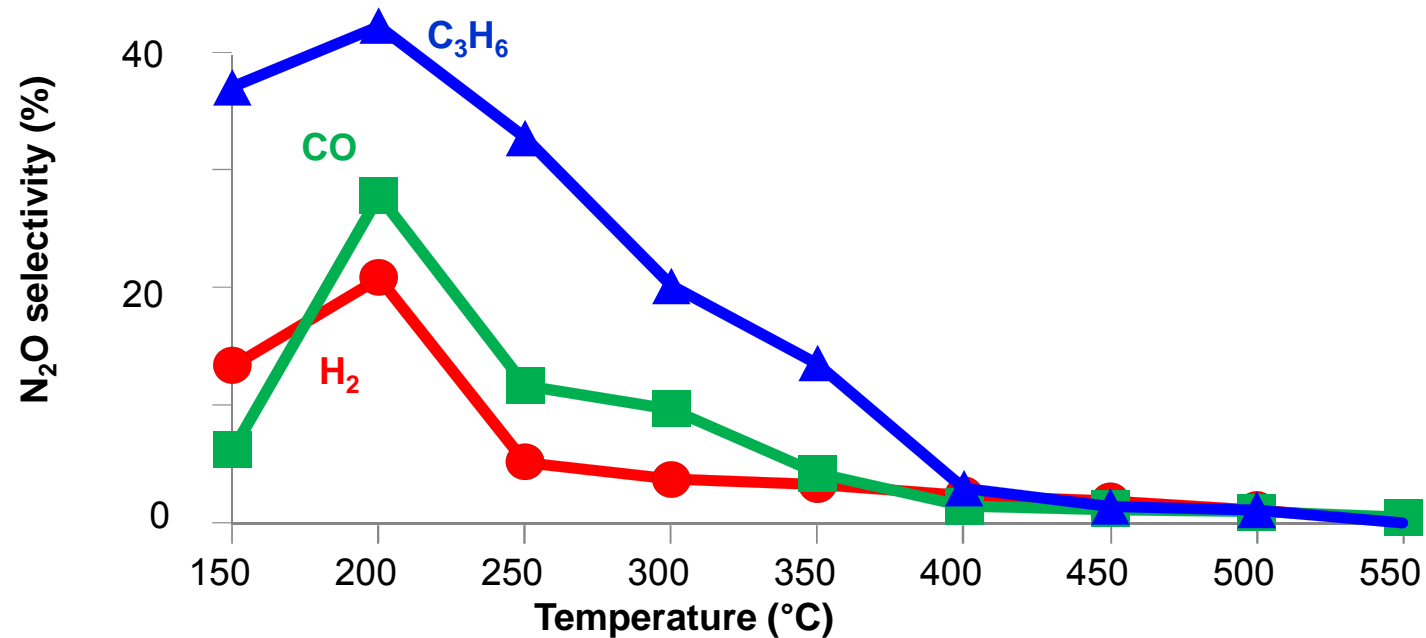


At 200 C self-inhibition of the reaction is observed as well as secondary N₂O peak after switching to inert atmosphere – probably NH₄NO₃ formation and decomposition

Choi et al., Catalysis Today (2012)

However, is this a unique reaction, and is the NH₃ intermediate necessary for N₂O formation during LNT regeneration?

N₂O Selectivity in Short Cycles (Fast Regeneration)



Choi, Pihl et al. (ORNL), CLEERS LNT data

- N₂O by-product formed at lower T with all reductants, particularly C₃H₆ >> CO > H₂. The unique NH₃ intermediate route cannot explain the trend – C₃H₆ at lower temperatures gives practically no NH₃ but significant N₂O.

⇒ N₂O can be formed by interaction of stored NO_x with any reductant.

⇒ **Ammonia intermediate is not necessary.**

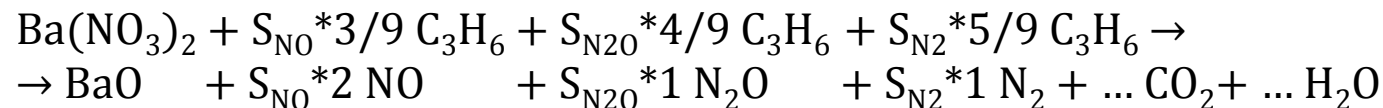
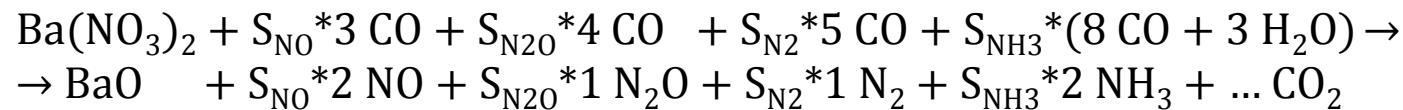
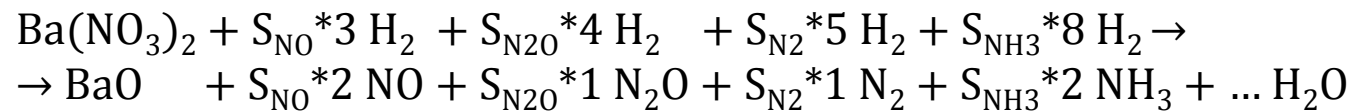
N₂O Source 3: Main N₂O Peak During the Rich Phase Generalized Approach to Reduction of Stored NO_x

Full range of N-products considered

Kočí et al. (2012),
submitted
to Topics in Catalysis

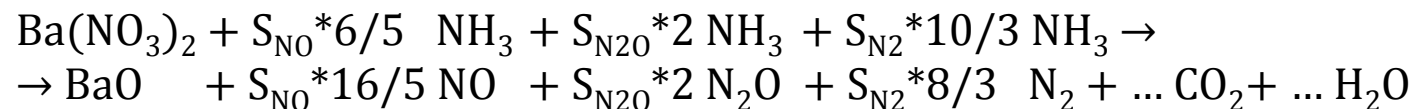
Reduction of stored NO_x (Ba sites in proximity of Pt)

Sum of selectivities ($S_{NO} + S_{N_2O} + S_{N_2} + S_{NH_3}$) = 1.0



Reduction of stored NO_x by NH₃ (Ba sites in proximity of Pt)

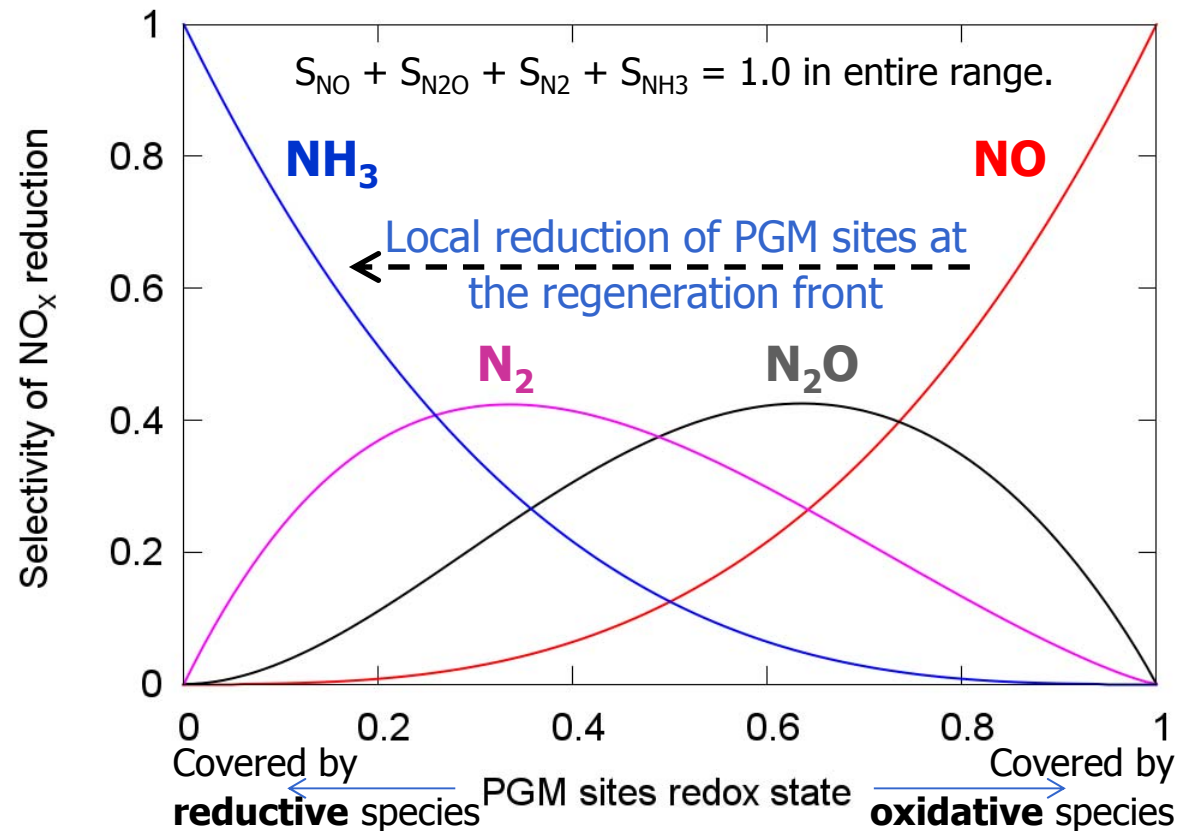
Sum of selectivities ($S_{NO} + S_{N_2O} + S_{N_2}$) = 1.0



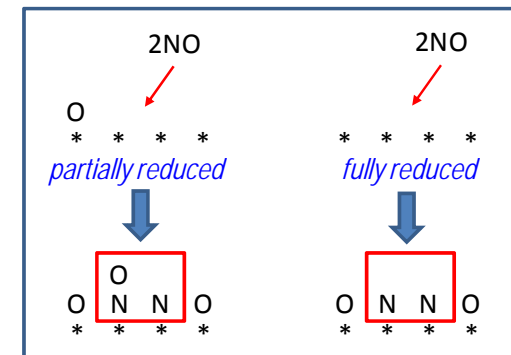
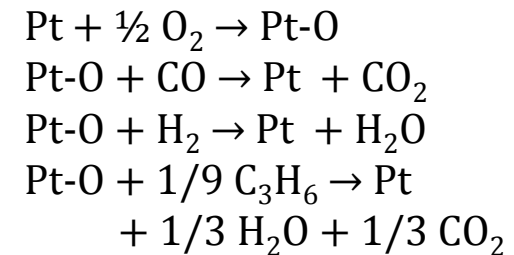
Can we have some approximate measure in global kinetic model that gives us prediction of actual local NO_x reduction selectivity?

Implementation of Variable Selectivity to Global Kinetic Model – Mapping to Local Pt (PGM) Sites State

- Local selectivities of the stored NO_x reduction to NO , N_2O , N_2 or NH_3 are linked with coverage of oxidative or reductive species on locally available PGM sites. Smooth polynomial functions are used and this approximate map is employed in global kinetics LNT model.

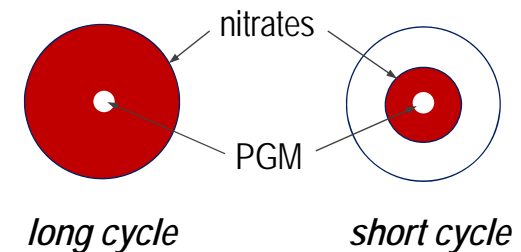


Simplified PGM state



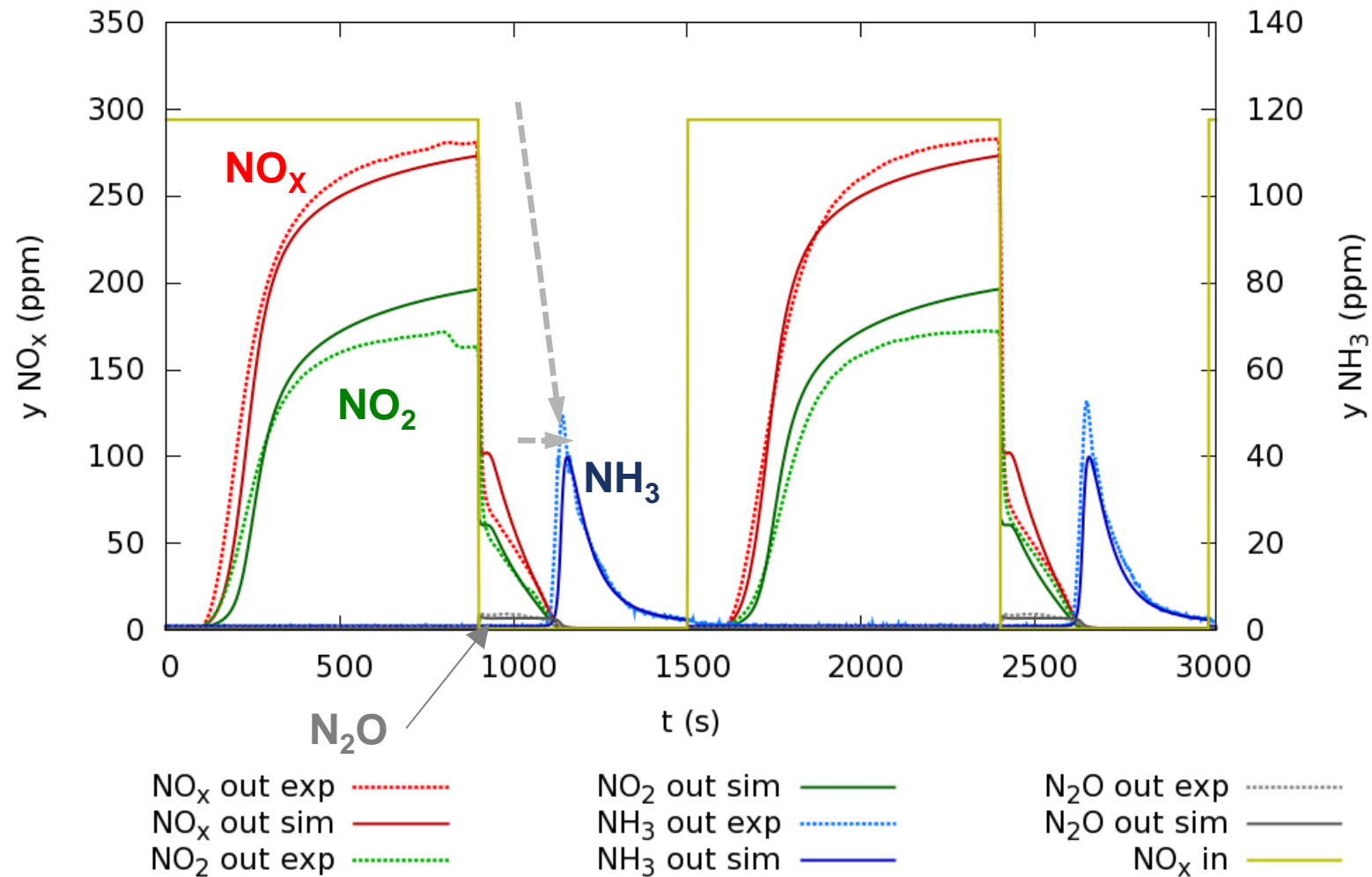
The model extension should allow to account for the main rates determining selectivity of NO_x reduction in LNT

- Three types of sites need to be reduced during the LNT regeneration:
 - NO_x storage sites
 - Oxygen storage sites
 - Precious group metal (PGM) sites
- Ratio between the respective reduction rates determines local selectivity:
 - If PGM reduction is slow and inefficient => higher N_2O formation
 - lower T
 - inefficient reductant of PGM (C_3H_6)
 - If PGM reduction is fast and efficient => N_2 , NH_3
 - higher T
 - efficient reductant (H_2)
 - Slower release of stored NO_x for reduction => NH_3
 - longer lean phase
 - NO_x adsorption on the storage sites farther from PGM redox sites
- Still, overall NH_3 yield is limited by internal NH_3 re-oxidation:
 - NH_3 formed in the reduced PGM zone is transported by gas convection to the oxidized zone, where it is consumed in reactions with the stored NO_x and oxygen.



Long Cycles (Slow Regeneration) – 300 C

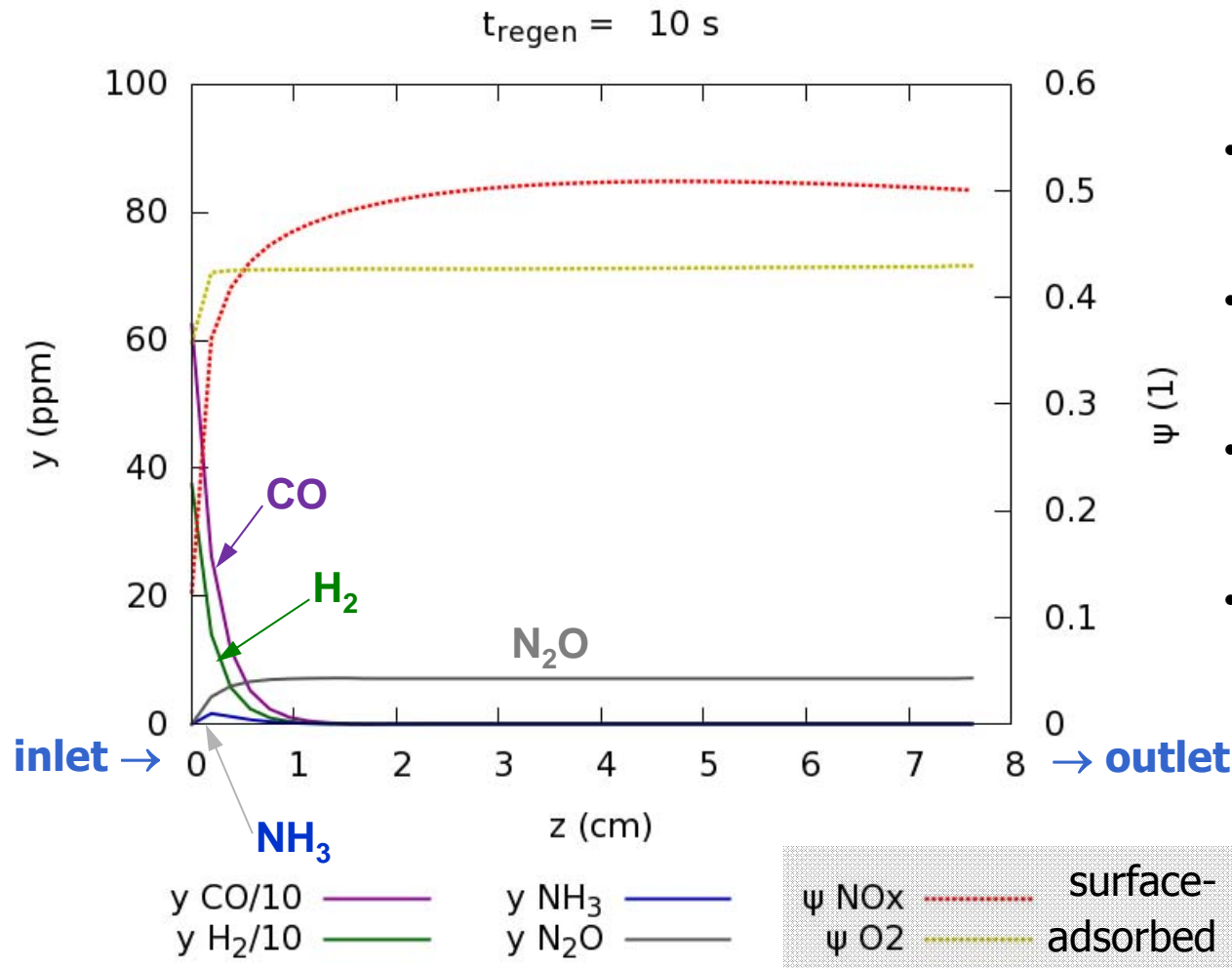
900 s lean + 600 s rich, slow regeneration by 625 ppm CO + 375 ppm H₂.



Evolution of Concentration Profiles during Regeneration

Moving reduction front.

Simulation results for a long cycle, slow regeneration by 1000 ppm (CO+H₂) at T=300 C.

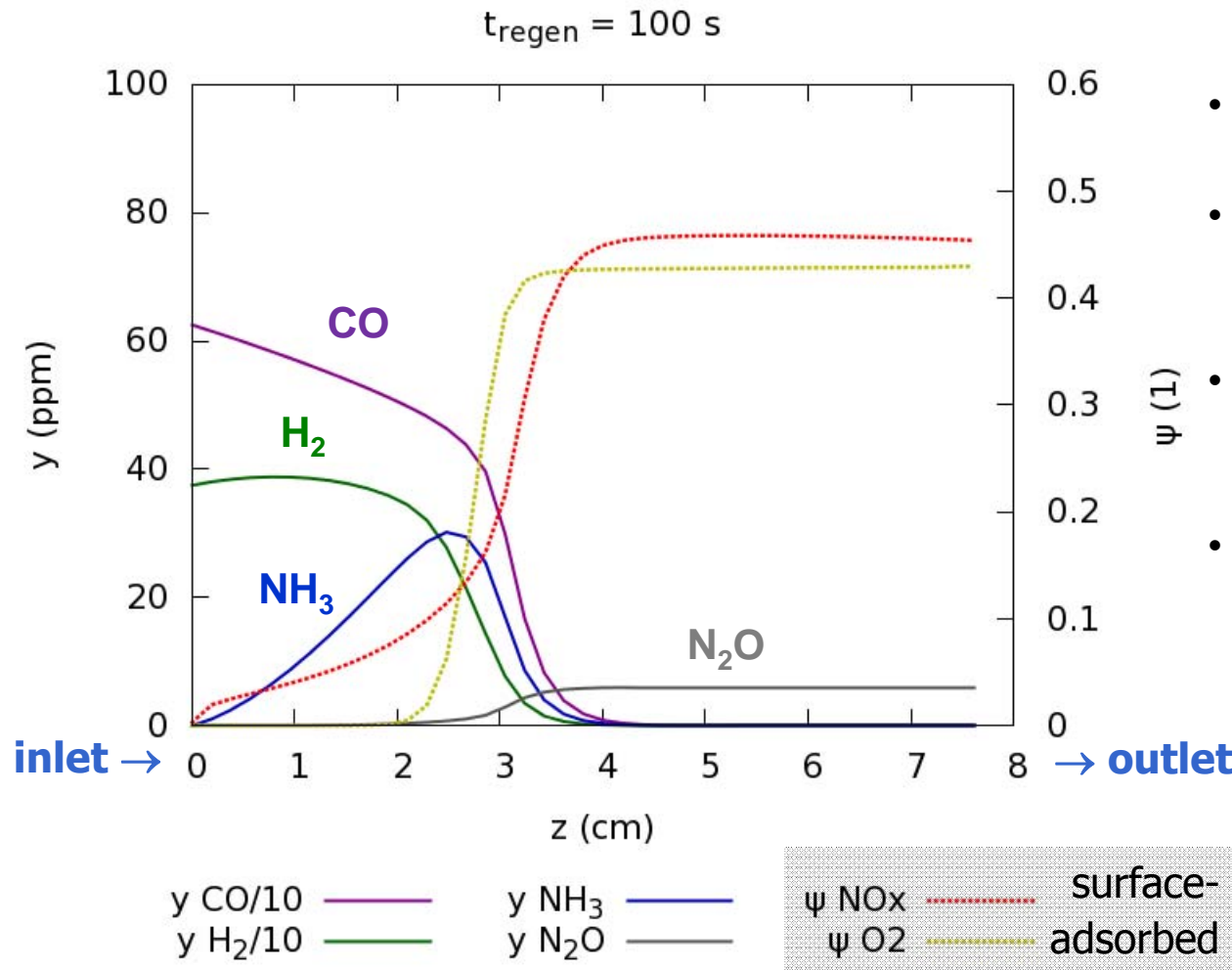


- Regeneration just begins at catalyst front
- Majority of catalyst is oxidized
- NH₃ formed in rich zone, readily re-oxidized
- N₂O observed at outlet

Evolution of Concentration Profiles during Regeneration

Moving reduction front.

Simulation results for a long cycle, slow regeneration by 1000 ppm (CO+H₂) at T=300 C.

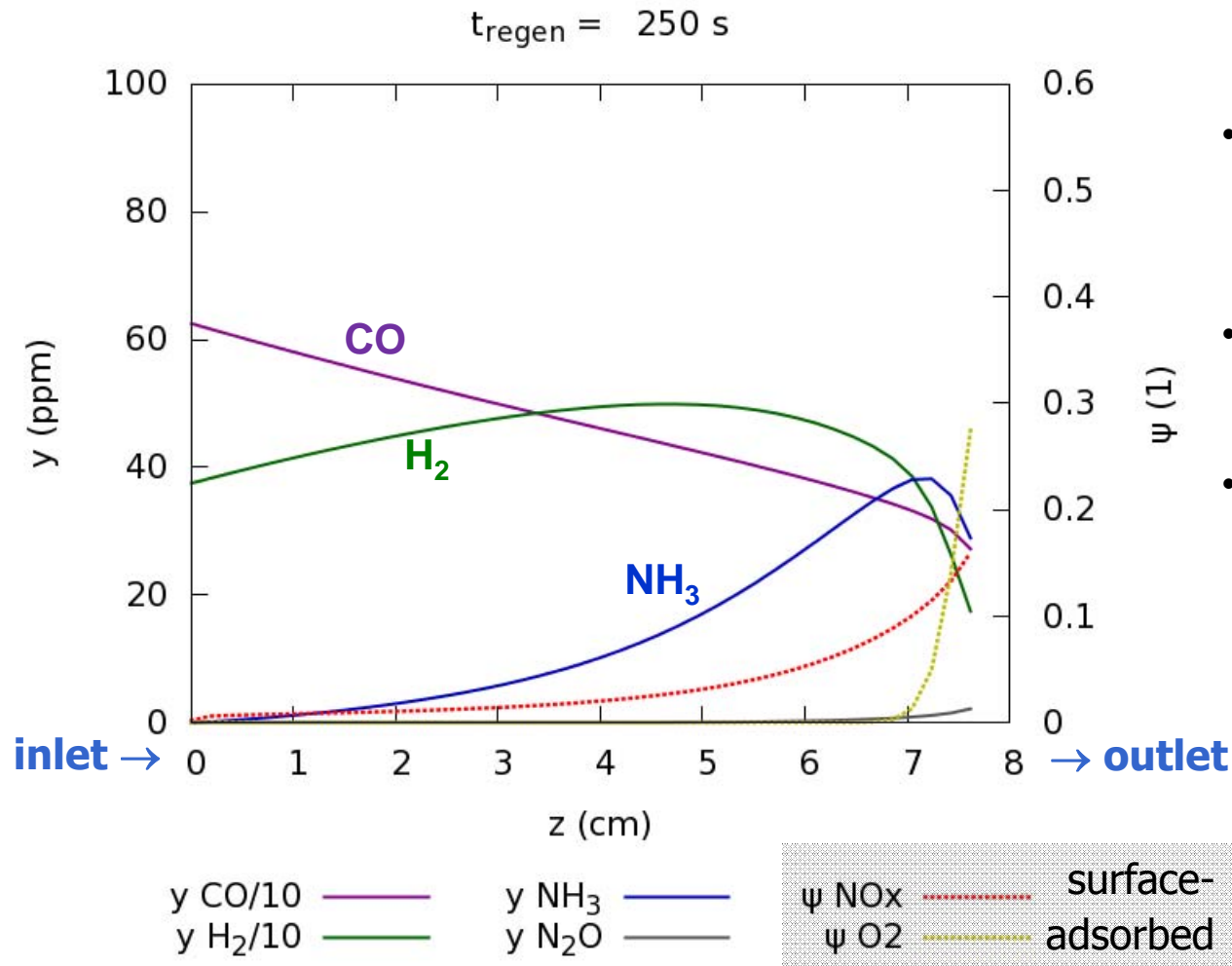


- Regen front at ~ 1/2 length
- Back 1/2 of catalyst is still oxidized
- NH₃ formed in rich zone , readily re-oxidized
- **Same N₂O** level at outlet
 - Formed at front of oxidized zone, then slipped through
 - Long lean phase leads to uniform surface NO_x & O₂
 - ⇒ Uniform N₂O as regen front sweeps through catalyst

Evolution of Concentration Profiles during Regeneration

Moving reduction front.

Simulation results for a long cycle, slow regeneration by 1000 ppm (CO+H₂) at T=300 C.

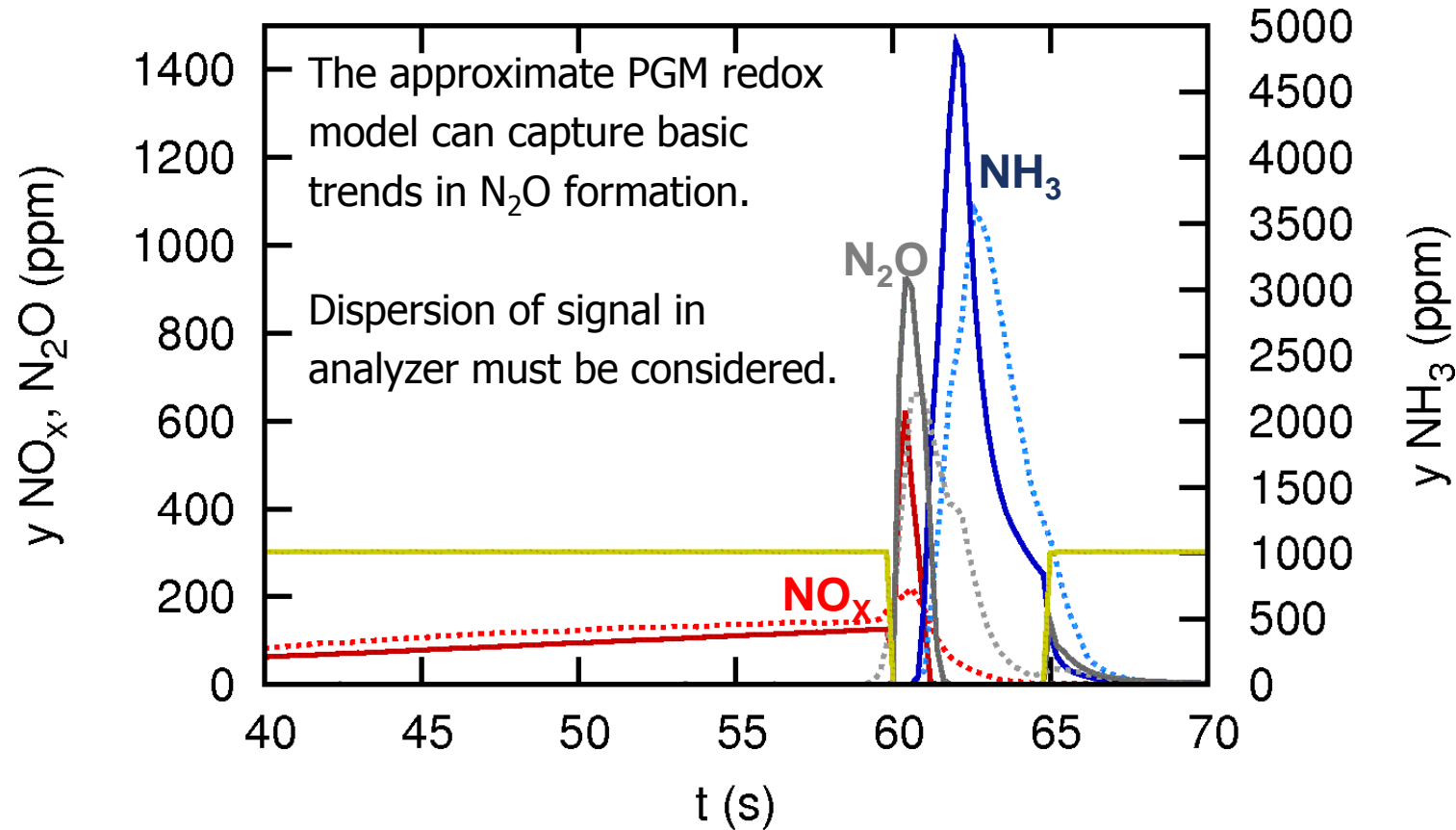


- Regen front at catalyst outlet
 - H₂ & CO breakthrough
 - NH₃ breakthrough
- NH₃ still formed only in rich zone
- N₂O drops to zero
 - Oxidized zone diminished

Short Cycles (Fast Regeneration) – 200 C, H₂ reductant

60 s lean + 5 s rich, fast regeneration by 3.4 % H₂

Slower NO_x release, slow PGM reduction ⇒ high N₂O, high NH₃.



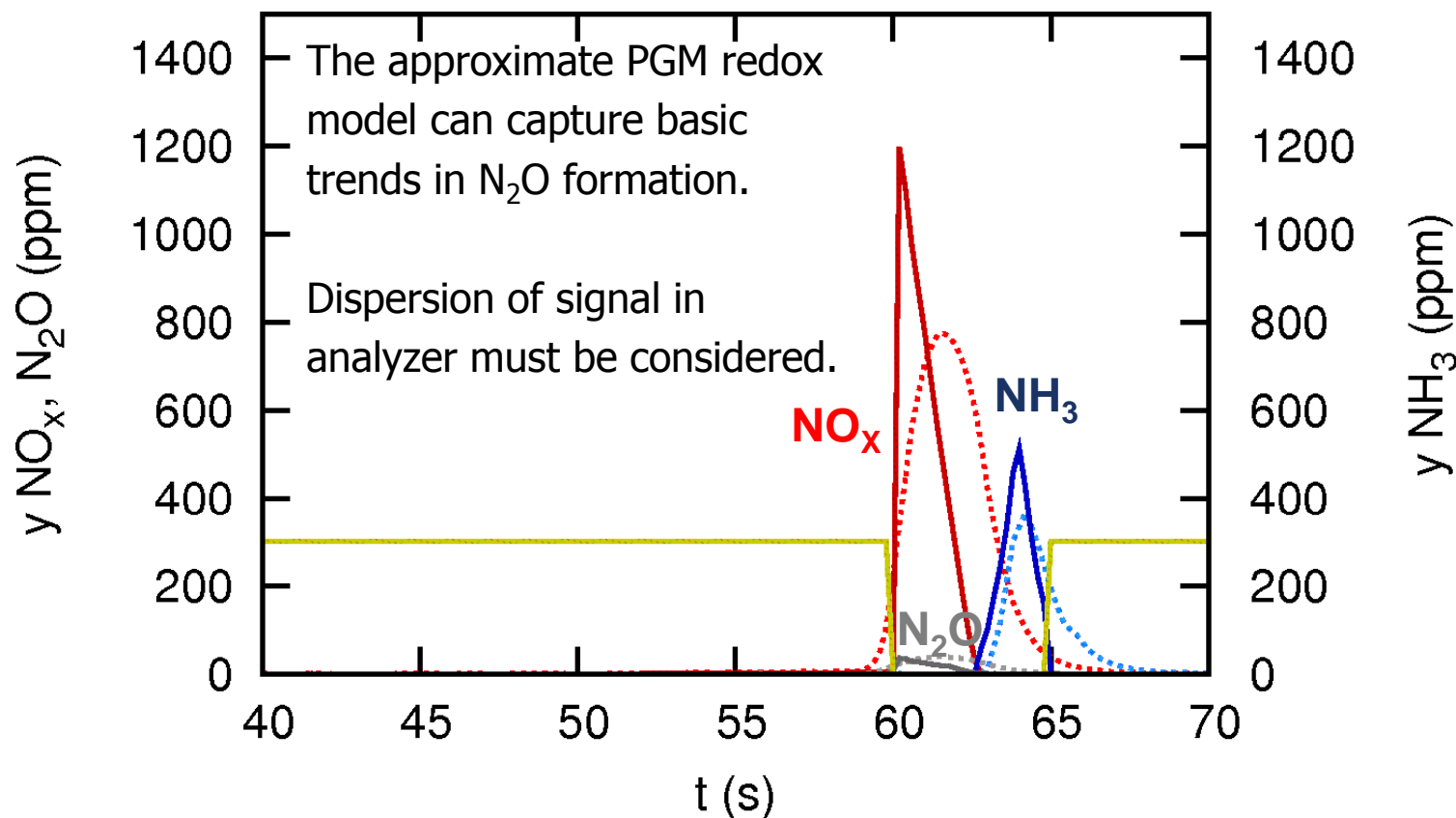
- | | | | | | |
|-------------------------|-------|--------------------------|-------|--------------------|---|
| NO _x out exp | | NH ₃ out sim | — | NO _x in | — |
| NO _x out sim | — | N ₂ O out exp | | | |
| NH ₃ out exp | | N ₂ O out sim | — | | |

Kočí et al. (2012),
submitted to Topics in Catalysis

Short Cycles (Fast Regeneration) – 400 C, H₂ reductant

60 s lean + 5 s rich, fast regeneration by 3.4 % H₂

Facile NO_x release, efficient PGM reduction ⇒ low N₂O, some NH₃ (changed scale).



NO_x out exp
 NO_x out sim ———
 NH₃ out exp

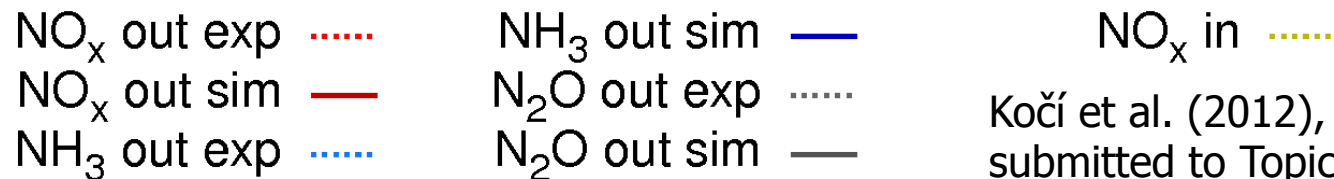
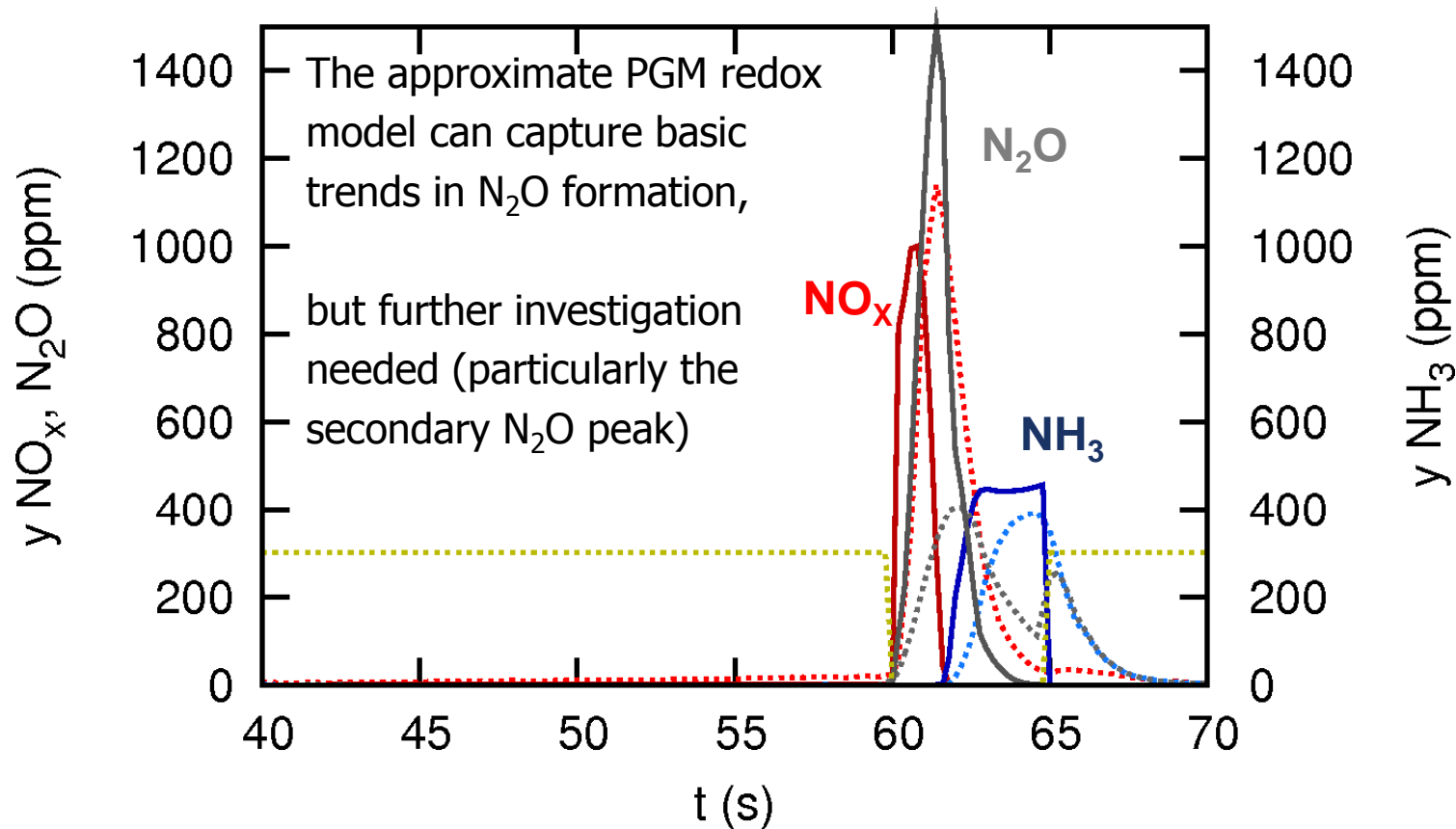
NH₃ out sim ———
 N₂O out exp

NO_x in ———
 Kočí et al. (2012),
 submitted to Topics in Catalysis

Short Cycles (Fast Regeneration) – 300 C, C₃H₆ reductant

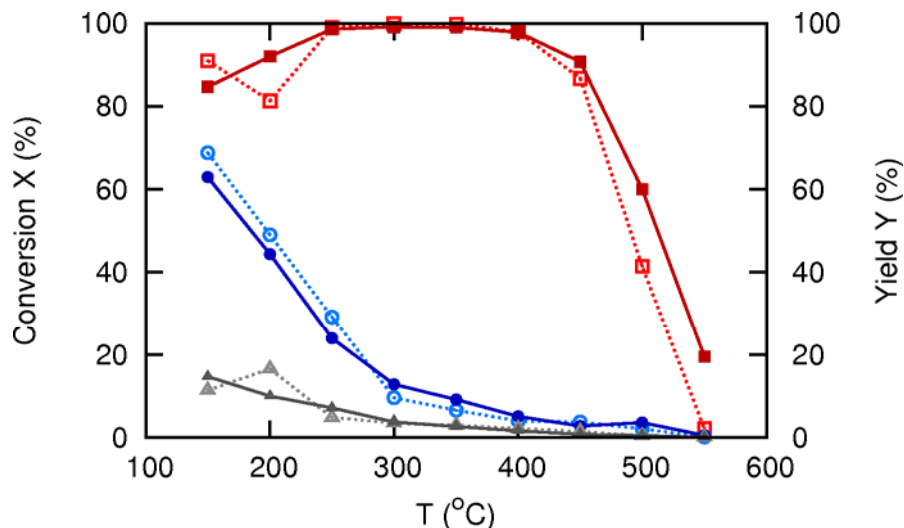
60 s lean + 5 s rich, fast regeneration by **3780 ppm C₃H₆**

Facile NO_x release, slow PGM reduction ⇒ high NO & N₂O, low NH₃.



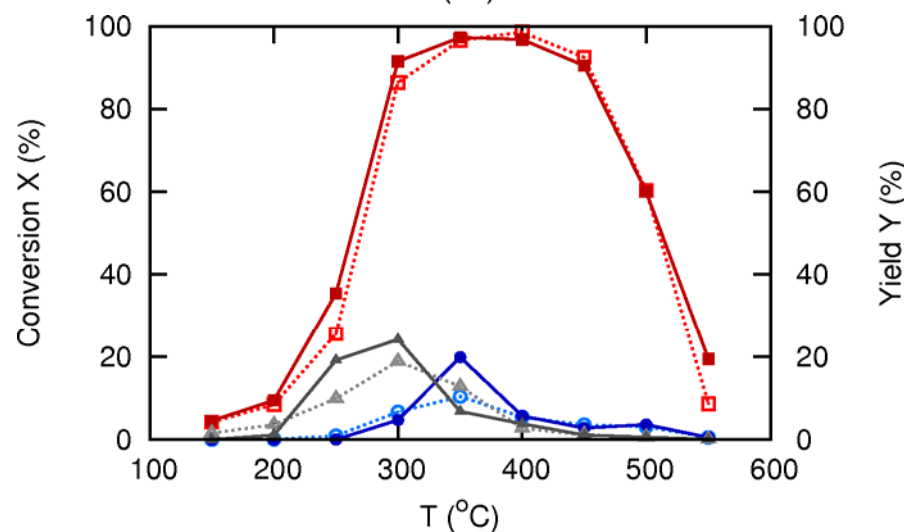
Kočí et al. (2012),
submitted to Topics in Catalysis

Integral Conversions & Yields – Short Cycles



Reduction by H₂

- Facile reduction of PGM sites
- Reduction of stored NO_x takes place already at 150 C
- Both NH₃ and N₂O yields reach maximum at lowest temperature and then decrease



Reduction by C₃H₆

- Inefficient reduction of PGM sites
- Poor NO_x conversion at low T
- High N₂O at 250-300 C, at the same time just a little or no NH₃
- NH₃ appears only above 300 C
- At 400 C and above similar to H₂

X NO_x exp ···■··· Y NH₃ exp ···○··· Y N₂O exp ···▲···
 X NO_x sim —■— Y NH₃ sim —○— Y N₂O sim —▲—

Kočí et al. (2012),
submitted to Topics in Catalysis

Is there an ideal LNT model?

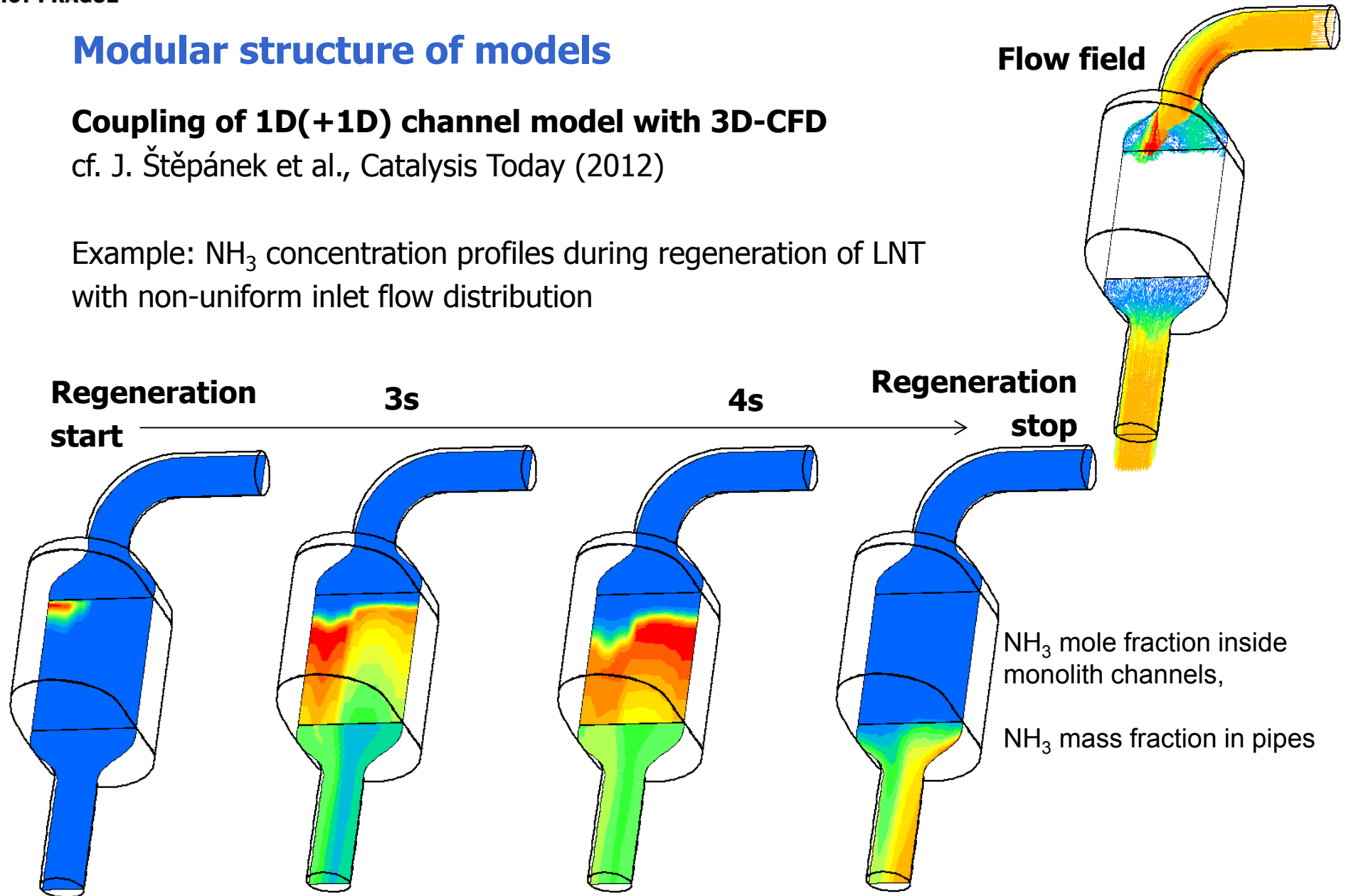
- **Catalyst manufacturers** optimize:
 - Catalyst formulation – reliable, fully predictive models are not available, DFT calculations etc. may indicate directions in still largely empirical research.
 - Catalyst distribution and coating morphology – the models involving detailed solution of internal transport effects (washcoat scale, pore scale, active particles scale) and mechanistic reaction kinetics can give the right answers.
- **Vehicle/engine manufacturers** optimize:
 - Design of combined aftertreatment system using existing, commercially available catalysts – a mix of global kinetic and simplified microkinetic models is used.
 - Fully formulated catalysts, realistic exhaust gas composition and wide range of operating conditions must be considered.
 - Conversions and selectivities to be predicted in dependence on actual transient cycle conditions in a quantitative manner.
 - Control and diagnostics – simplified models, however, spatial distribution effects difficult to lump.

Modular structure of models

Coupling of 1D(+1D) channel model with 3D-CFD

cf. J. Štěpánek et al., Catalysis Today (2012)

Example: NH_3 concentration profiles during regeneration of LNT with non-uniform inlet flow distribution



Concluding remarks

- Validated catalyst models can speed up design and testing of current and future combined exhaust gas after-treatment systems.
- Various LNT models emphasize different aspects but share similar principles.
- Criteria for model selection:
 - Purpose of the model use
 - Model development and fitting costs
 - Computation time costs

Acknowledgements

Co-workers and students from research group Monolith, ICT Prague
www.vscht.cz/monolith

Daimler AG

Oak Ridge National Laboratory FEERC – Jae-Soon Choi, Bill Partridge, Josh Pihl
US DOE Vehicle Technologies program, CLEERS

Czech Ministry of Education, Kontakt II project LH 12086